A RAND NOTE

CALCULATION OF RADIATED SIGNALS FROM HIGH-ALTITUDE NUCLEAR DETONATIONS BY USE OF A THREE-DIMENSIONAL DISTRIBUTION OF COMPTON ELECTRONS

Cullen M. Crain

March 1982

N-1845-ARPA

Prepared For

The Defense Advanced Research Projects Agency

Rand
SANTA MONICA, CA. 90406

APPROVED FOR PUBLIC RELEASE; DISTRIBUTION UNLIMITED

A RAND NOTE

CALCULATION OF RADIATED SIGNALS FROM HIGH-ALTITUDE NUCLEAR DETONATIONS BY USE OF A THREE-DIMENSIONAL DISTRIBUTION OF COMPTON ELECTRONS

Cullen M. Crain

March 1982

N-1845-ARPA

Prepared For

The Defense Advanced Research Projects Agency

Rand
SANTA MONICA, CA. 90406

APPROVED FOR PUBLIC RELEASE; DISTRIBUTION UNLIMITED

PREFACE

The method of calculating the electromagnetic pulse (EMP) produced by a high-altitude burst, as presented in this Note, was originally discussed at the Joint EMP Technical Meeting--First Annual Nuclear EMP Meeting, held at the Air Force Weapons Laboratory in September 1973, in a paper by the author entitled *A Numerical Example of the Effect of Atmospheric Scattering on Predicted EMP Environments*. Several requests for a more detailed version of the method were received from attendees at the meeting. During the following years a number of detailed comparisons were made by the author and the Air Force Weapons Laboratory (AFWL/DYT) of calculated electromagnetic pulse environments from specified bursts using the author's method and the AFWL's CHEMP code. When the same input parameters were incorporated into the calculations, the numerical agreement in the pulse amplitude versus time was excellent--typically within about 25 percent at times of principal interest, i.e., to times well past the time of maximum pulse amplitude.

This Note should be of interest to analysts involved with EMP environmental predictions and also to those desiring additional physical insight into the generation of the EMP signal and how it is influenced by the gamma source time characteristics, by atmospheric scattering, and by residual ionization of the atmosphere. It is being published at this time to make available to those concerned with EMP environments an alternative and physically descriptive method for determining EMP levels. It contains the unclassified general theory and analysis portions of a more extensive classified report of the same title published in 1974.

The Note was prepared under the sponsorship of the Defense Advanced Research Projects Agency's study project "Future Strategic Communications Systems and Nuclear Survivability Issues."

SUMMARY

This Note presents the essential details of a three-dimensional method of calculating the radiated electromagnetic signal that is caused by magnetic deflections of a distribution of Compton electrons produced in the upper atmosphere by prompt gamma radiation from a high-altitude nuclear detonation or a series of detonations. The method differs from that previously developed for such calculations in that the solution is obtained from summing the radiation fields from the individual electrons in a three-dimensional volume instead of combining the individual electron motions to determine a time- and space-dependent current from which the radiation field is evaluated using a one-dimensional approximation to the solution of Maxwell equations.

In the Note the effects of the time characteristics of the source gamma (γ) output, the effects of atmospheric scattering in reducing the coherent radiation from the Compton electrons, and the effect of residual atmospheric ionization (preionization) in reducing the observer signal amplitude are developed and illustrated numerically.

The three-dimensional characteristics of the source are brought out in illustrative numerical examples. These examples give additional physical insight into the source characteristics and demonstrate the importance of scattering and atmospheric ionization, when present, in influencing the EMP amplitude/time characteristics.

CONTENTS

PREFACE iii

SUMMARY v

Section
I. INTRODUCTION 1

II. DETAILS OF THE SUMMED ELECTRON-FIELD METHOD 3
A. General Discussion 3
B. Illustrative Calculation Using a Delta-Function γ Source and Ideal Circular-Orbit Electrons 14
C. Time-Dependent γ Source Calculations 19
D. Effects of Inclusion of Atmospheric Scattering of Compton Electrons 24
E. Effects of Inclusion of Absorption Effects from Residual Ionization and Self-Ionization 32
F. Summary Comments on Summed Electron-Field Method 42

REFERENCES 45

I. INTRODUCTION

The purpose of this Note is to outline and numerically illustrate the essential details of a fully three-dimensional method of calculating the radiated electromagnetic signal from magnetic deflections of a distribution of Compton electrons produced in the upper atmosphere by prompt gamma radiation from a high-altitude nuclear detonation. The three-dimensional method evaluates the radiation fields (at a given time) from individual electrons. It uses Lienard-Wiechert potentials and sums the fields from all the spatially distributed electrons which contribute to the observer field at the given time. Repetition of the process for various times after the detonation leads to the full determination of the signal amplitude as a function of time. The method outlined--development of the solution in terms of the radiation field from an individual electron--is different from the method which has been generally employed for calculation of the radiation. In previous solutions,[1] the method has been to combine the motions of all Compton electrons to determine a time- and space-dependent electric current and then to calculate the radiation from this current. Both methods, properly applied, must give the same answer for the radiation field from a given Compton electron configuration, since both are derived from Maxwell's equations. A formal proof of this has been given by Sollfrey[2] for the zero conductivity case.

As will be shown, summing the fields of the individual electrons requires relatively little computational effort and readily permits the inclusion of atmospheric scattering and absorption effects in the solution. Atmospheric scattering was not considered in Ref. 1 but has been shown[3,4] to be, in general, an important factor in determining the radiation field. Also, the present method provides additional physical insight into the process of generation of the radiated electromagnetic pulse (EMP) arising from the magnetic deflection of Compton electrons.

Section II of this Note gives details of the principal steps of the electron field summation method of EMP calculation. For simplicity in

presenting the method, vertical geometry and a magnetic field perpendicular to the burst/observer path are used, and numerical values are illustrated for all steps in the development of the method.

II. DETAILS OF THE SUMMED ELECTRON-FIELD METHOD

A. GENERAL DISCUSSION

Figure 1, assuming vertical geometry, shows the geometrical aspects of the summed electron-field method. A short burst of γ radiation is emitted by a source well above the altitude where the emitted γ radiation effectively interacts with the atmosphere. The γ radiation impinges on the atmosphere below the burst and produces Compton electrons which deflect in the earth's magnetic field and radiate an electromagnetic signal which travels to the observation point. The electromagnetic pulse is determined at an illustrative location directly below the burst by appropriately summing the time-dependent electric fields produced at the observation point by all the electrons in the ellipsoidal volume that can contribute at a given time. In the calculation, the time-dependent effects of atmospheric scattering on the field produced by the electron are explicitly included, as is the reduction in the field caused by absorption by secondary ionization, which exists between a given electron and the observation point.

The first signal reaches the observer at the time R/C (C = velocity of light) after the first γ radiation from the burst. This signal results from Compton electrons produced on the direct path between the burst and the observer. The ellipse, much shortened in Fig. 1, illustrates the boundary of the ellipsoid of revolution about the burst/observer axis that contains all the radiating electrons that can contribute to the observer field at a time t - R/C, or τ, after arrival of the first signal. It is easily shown that the length of the axis, X, of the ellipsoid at an axial distance r_1 from the burst and r_2 from the observer is

$$X = \left(\frac{2C\tau r_1 r_2}{r_1 + r_2} \right)^{\frac{1}{2}} \tag{1}$$

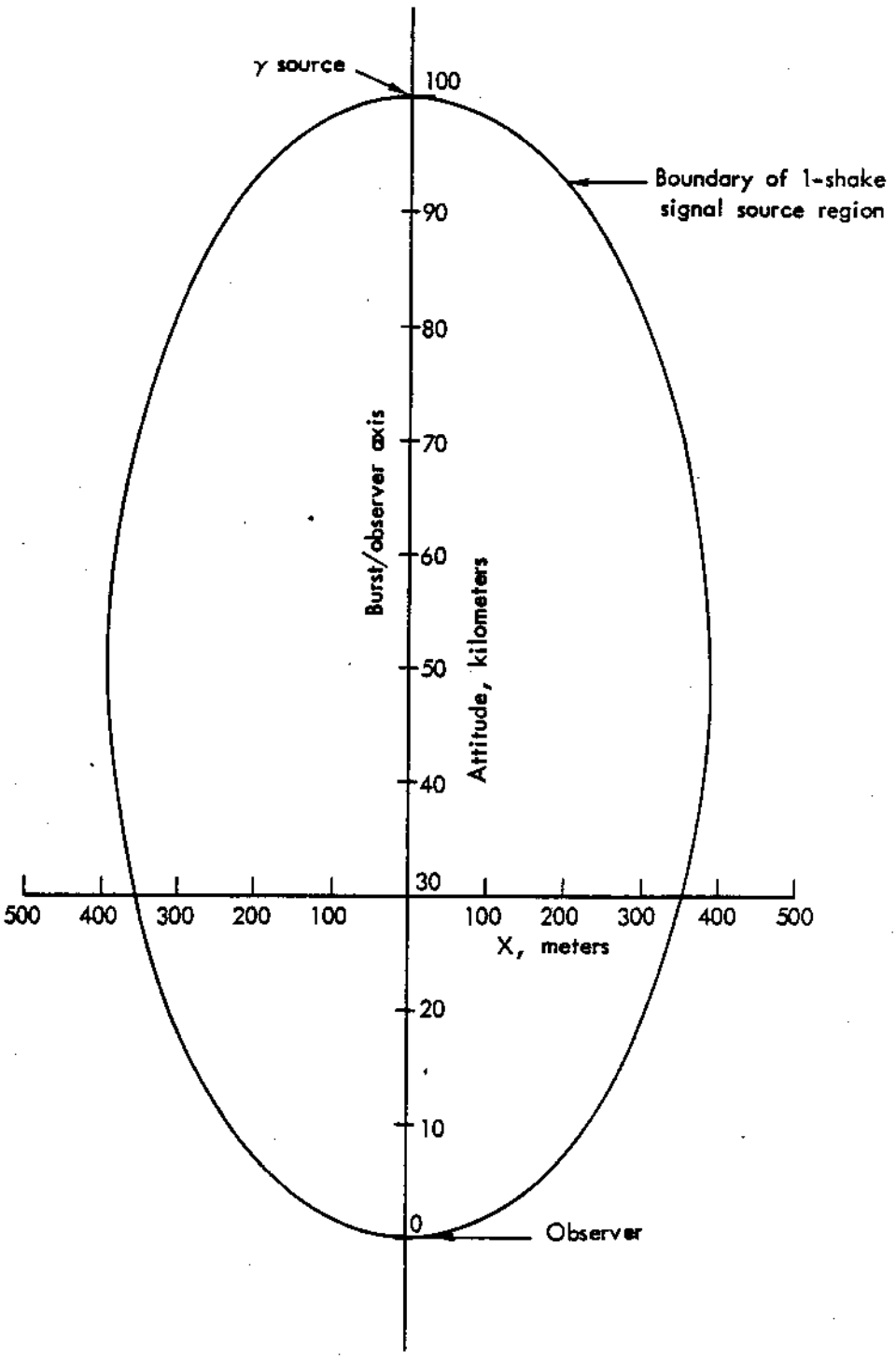

Fig. 1 – Geometrical factors for 100 km burst and ground observer (vertical path)

To illustrate the dimensions of the problem, let

$R = r_1 + r_2 = 10^5$ meters

$\tau = 10^{-8}$ seconds or 1 shake

$r_1 = 7 \times 10^4$ meters

$r_2 = 3 \times 10^4$ meters

Then

$X = 355$ meters

or any time τ, in shakes,

$X = 355\sqrt{\tau}$ meters.

Consider a disc whose radius is X, as shown in Fig. 1. Clearly, at times up to about 10^{-6} seconds (or 100 shakes), the dimension X is very small relative to the distance of the disc from the burst or to the observer. Hence the γ flux from the burst can be considered constant across the disc.

The γ flux at a given height and the number of first scattered Compton electrons produced at this height are readily calculated by use of total mass attenuation coefficients for air, such as those given by Evans,[5] and a standard reference atmosphere.[6] For any arbitrary γ spectral distribution, the γ spectrum can be divided into several small segments with an appropriate average γ energy per segment. The Compton electron production for each segment is evaluated by means of the procedure of the monoenergetic calculation. The total Compton production is then the sum of the Compton electrons produced by the several segments. Figure 2 illustrates the height distribution of Compton electrons produced by a prompt γ source of 0.01 KT yield. The figure portrays vertical geometry, a burst height of 100 km, and a source emitting 1.6-MEV monoenergetic γ radiation. Also shown on Fig. 2 are the height distributions of total secondary electron density production (N_∞) and the electron density production due only to the first generation Compton electrons (N_1).

The Compton electrons produced by Compton scattering of γ radiation of a given energy have initial energies and directions as given

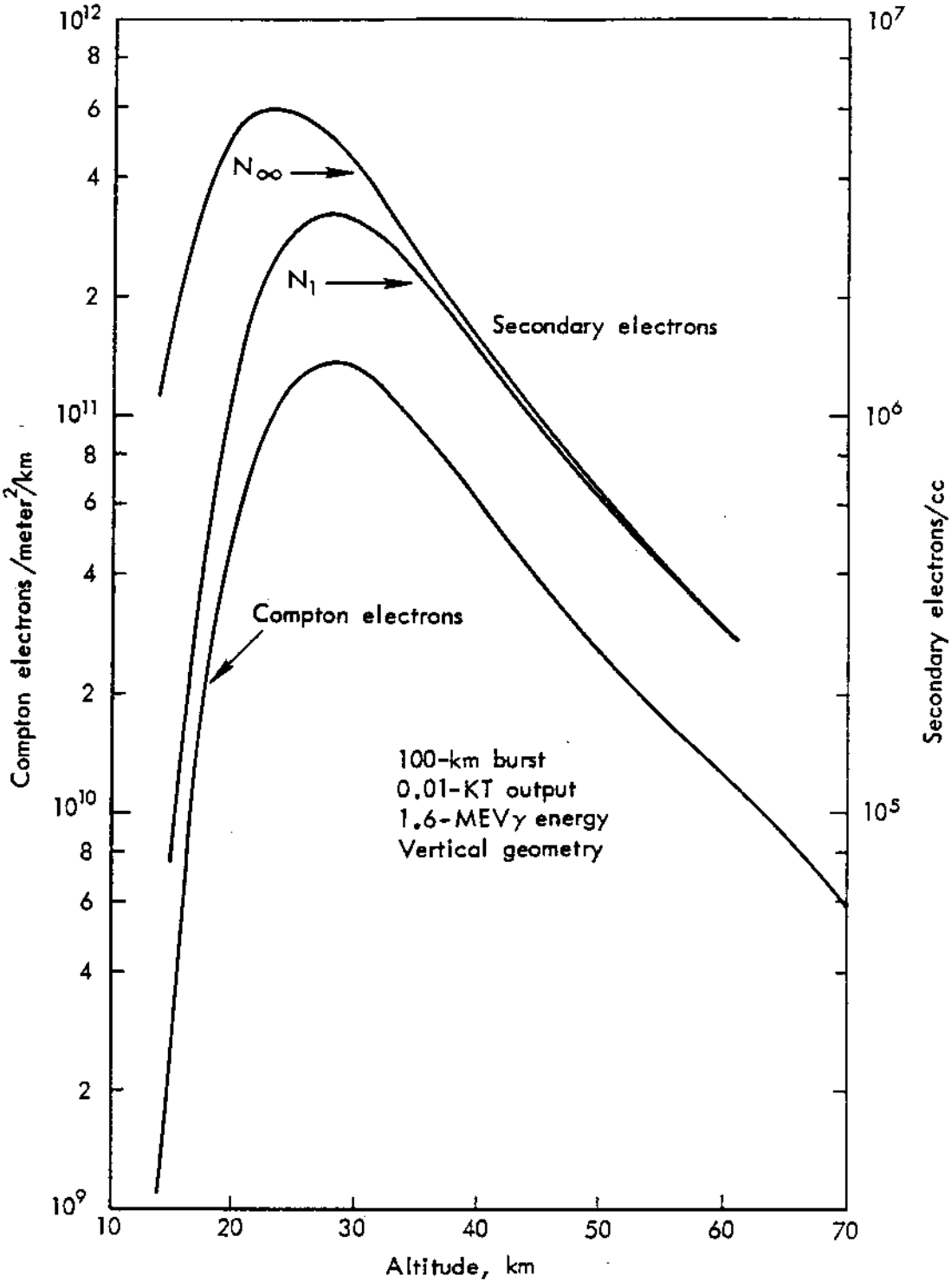

Fig. 2 — Compton electron production vs height

by the Klein-Nishina formulas.[5] Figure 3 illustrates the electron energy and relative number per unit angle as a function of angle from the burst/observer axis for 1.6-MEV γ radiation. For observer times (i.e., true signal time at the observer location) of principal interest (a few shakes) and typical EMP geometry such as that in Fig. 1, the initial distributions shown in Fig. 3 are essentially constant throughout the ellipsoid, since the angle between the line from the edge of the disc to the observer and the burst/observer axis is small. In the analysis in this Note the initial distributions shown in Fig. 3 are assumed to apply throughout the Compton electron source region, confined to the ellipsoidal region of Fig. 1. This assumption results in an overestimate of the radiated signals that is negligible at early times but increases with time.

Rather than deal with the radiation from electrons that have number versus angle and energy distributions as shown in Fig. 3, it is convenient in both the summed electron-field method and the continuum-current method of Ref. 1 to replace the distributions by equivalent forward-directed electrons that will produce the *same initial field intensity* at the observation point as is produced by the distribution of electrons.

Since the initial number and the energy distributions of electrons are known from the Klein-Nishina formulas, one may precisely evaluate the normalized initial field produced by this distribution at the observation point by summing the fields of all the electrons in the distribution. The field, at a distance r, due to a relativistic electron with angle θ to the direction of the observer and with a velocity βC perpendicular to a magnetic field B is given by Lienard-Wiechert potential theory (see any text on electrodynamic theory; e.g., Ref. 7) and in simple form is

$$E = \frac{e^2 \beta \, (\cos \theta - \beta) \, B \, (1 - \beta^2)^{\frac{1}{2}}}{4\pi m_o \varepsilon_o C r (1 - \beta \cos \theta)^3} \qquad (2)$$

where e is the electron charge, m_o is the rest mass, ε_o is the permittivity of free space, and C is the velocity of light.

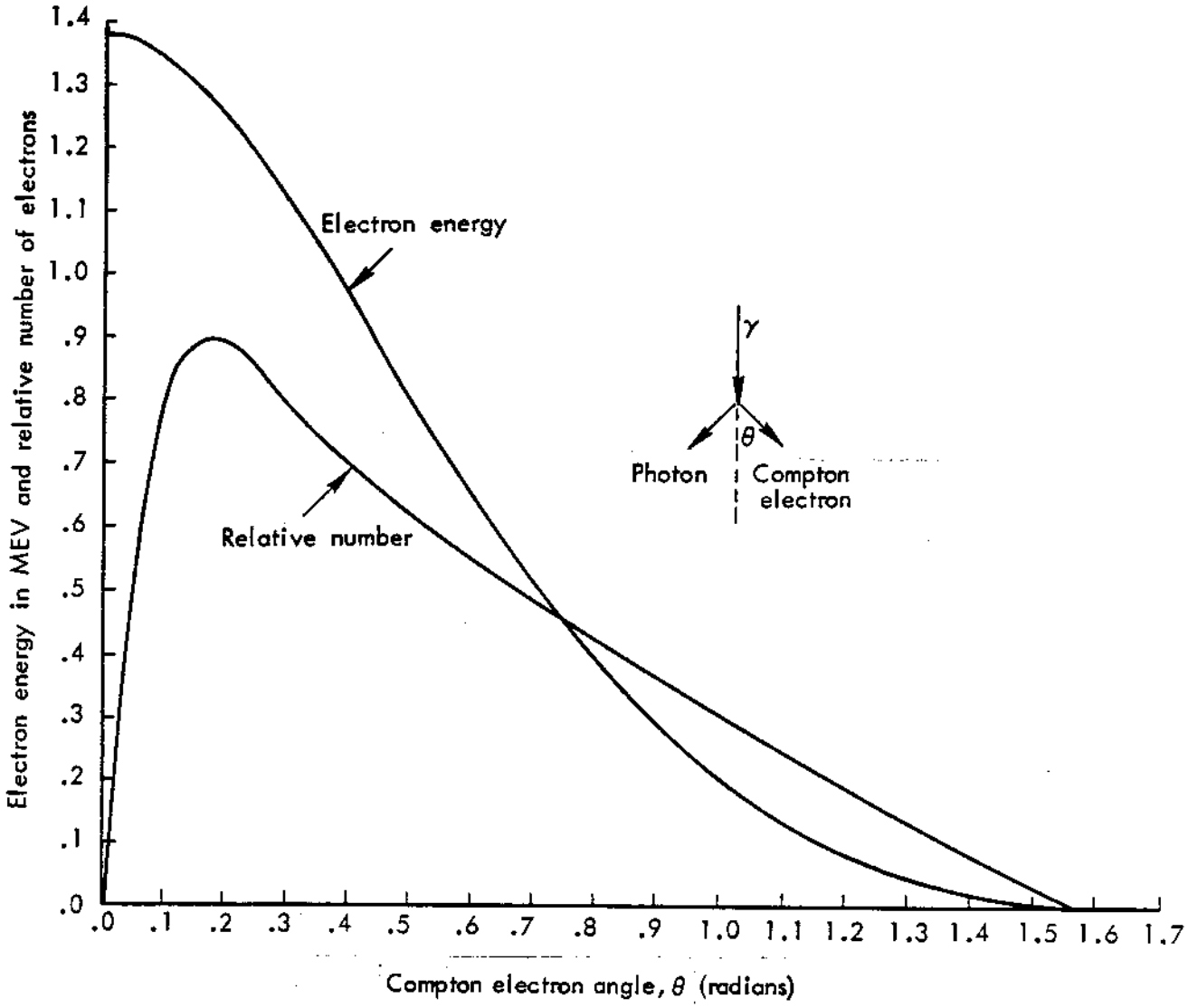

Fig. 3 — Energy and number distribution for Compton scattering: 1.6-MEV γ

The field is normal to the line between the electron and the observer in the direction of the electron's acceleration caused by the perpendicular component of the steady magnetic field. Figure 4 shows the distribution of the contributions to the observed radiation field as a function of the initial angle θ of the Compton electrons (as in Fig. 3). For Fig. 4, a magnetic field perpendicular to the direction of the γ ray was used, and the fields were evaluated for all electrons in the cone at an angle θ; the area under the curve is proportional to the total field contributed by the distribution. Again using the Lienard-Wiechert relation, we can readily calculate the velocity or energy of that number of forward-directed electrons which will produce exactly the same initial field intensity at the observation point as the ensemble of Klein-Nishina distributed electrons. For 1.6-MEV γ radiation, the equivalent forward electron is determined by this process to have a β of 0.87 or an energy of 0.53 MEV. This value is to be contrasted with the average Compton electron energy of 0.8-MEV which, if used, greatly overestimates the observer field.

Figure 5 shows a plot of the energy of equivalent forward-directed electrons versus incident γ energy for a range of γ energies. Calculations for Fig. 5 were performed as illustrated above for 1.6-MEV incident γ radiation.

The above analysis applies to the field intensity of electrons before they have been rotated by the magnetic field and gives precisely the correct result for electrons of zero age. Sollfrey[8] has extended the above analysis by comparing as a function of time the observer field intensity due to the rotated ensemble of Compton electrons with that from the rotated equivalent forward-directed electrons. His analysis shows that, for the times of primary interest in EMP, the field versus time due to the rotated equivalent electrons is practically the same as that due to the rotated ensemble of Compton electrons. Thus the approach of using equivalent forward-directed electrons is quite accurate and provides a significant reduction in the computational effort. Again it should be emphasized that the energy of the equivalent forward electron for producing the correct observer field is significantly smaller than the average electron energy of the Compton electrons.

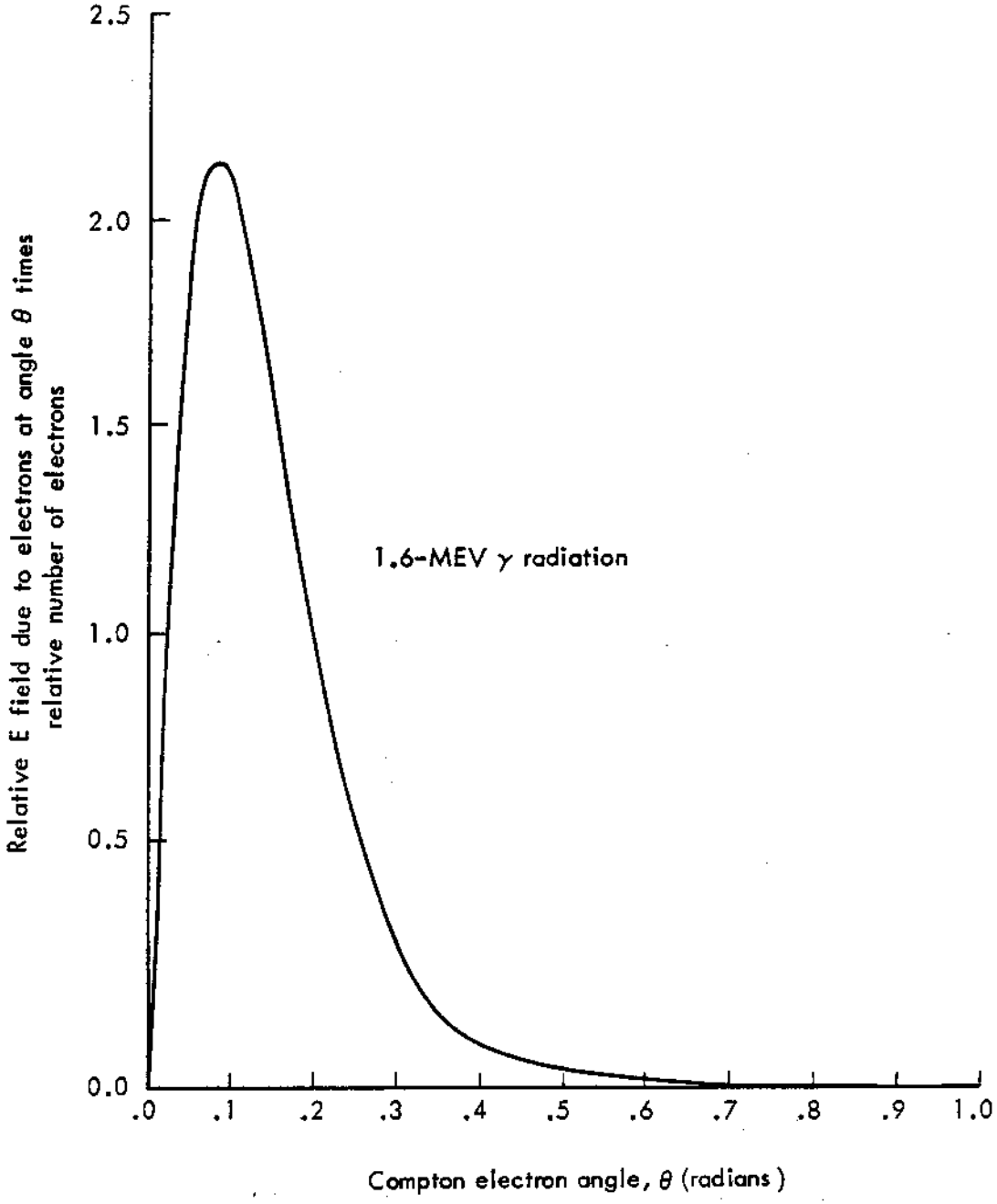

Fig. 4 — Relative radiated field vs angle for Klein-Nishina distributed Compton electrons

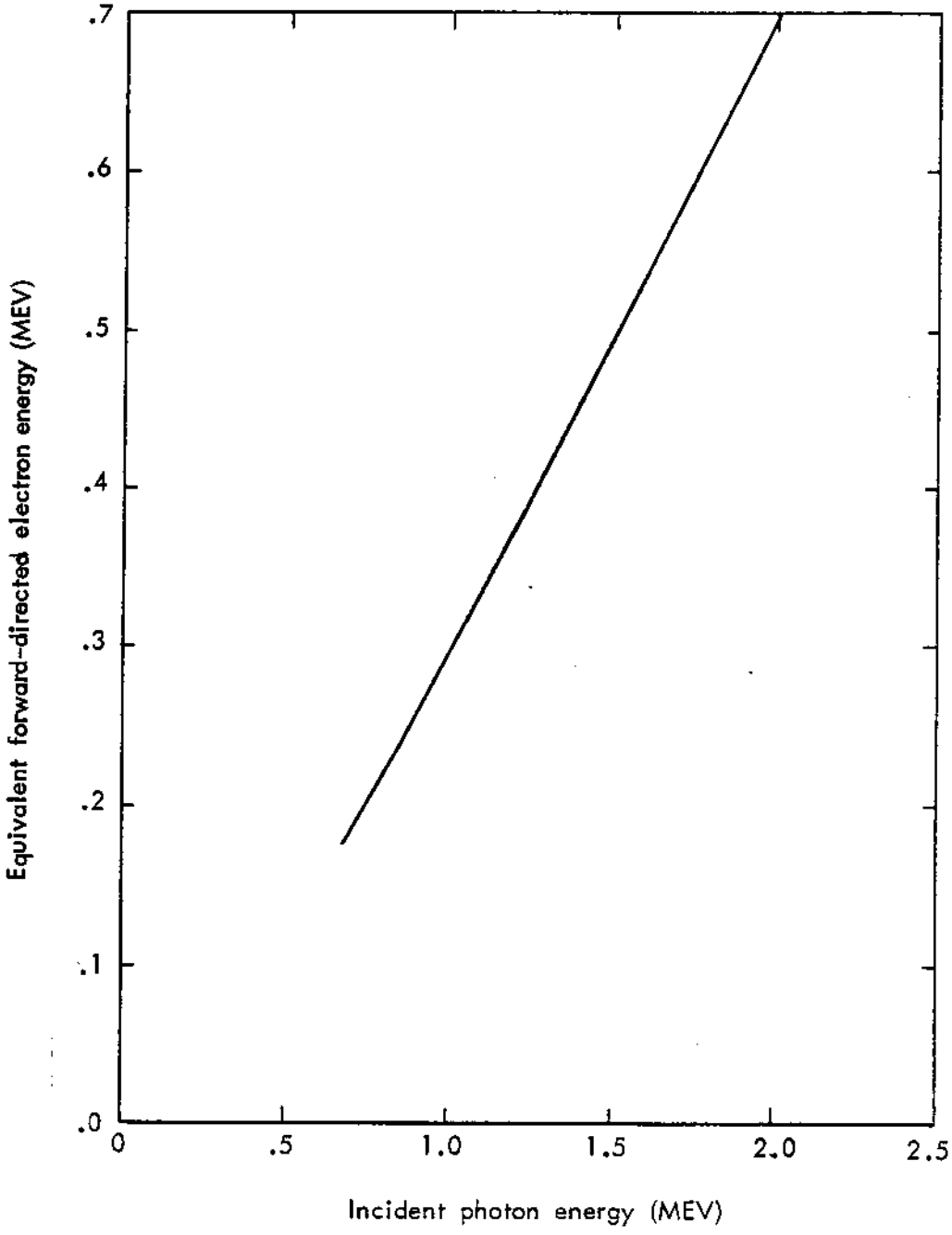

Fig. 5 — Energy of equivalent forward electron vs incident photon energy

This is true for either the summed electron-field approach or the continuum-current approach in EMP calculations.

Having determined (1) the height distribution of the first-scattered Compton electrons which results from a given γ impulse and specified burst/observer geometry and (2) the equivalent energy of forward-directed electrons that produce the same field as the Klein-Nishina distribution of Compton electrons, we can proceed to determine the observer field arising from the full three-dimensional distribution of Compton electrons.

Figure 6 shows, for a thin layer of Compton electrons in the height region where they are produced by the γ radiation from the source (as in Fig. 2), the burst/observer axis and the outer boundary of the disc from which the field of radiating electrons can contribute to the observer radiation field at a time τ, where τ is simply the difference between travel time at the velocity of light from the burst to the observer along the burst/observer axis and travel time along the path to the outer edge of the disc. As was discussed above, the Compton electrons, which have a distribution of energies and directions, can be replaced for purposes of determining the radiation field at the observation point by equivalent initially forward-directed electrons of appropriate energy. For the moment, to aid in understanding Fig. 6, consider the γ radiation to be emitted instantaneously, i.e., as a delta function. At the edge of the disc, the electrons that contribute to the observer field at time τ have a velocity parallel to the burst/observer axis (since the disc radius, X, is very much smaller than the burst/observer distance, shown on Fig. 1). Electrons along the burst/observer axis have been turned because of acceleration by the magnetic field and have acquired a direction determined by the amount of turning in a time τ. The electrons between the axis and the outer edge of the disc have been turned for times intermediate between 0 and τ and have velocity directions as illustrated. Consider the intermediate path to electron "q" shown by the dashed lines in Fig. 6. The relative γ radiation travel time to "q" plus the relative travel time of the signal radiated by the electron to the observer is less than τ, say $\tau - \Delta\tau$. Thus the electron "q" has rotated for a time $\Delta\tau$ when it makes its contribution to the observer field at time τ.

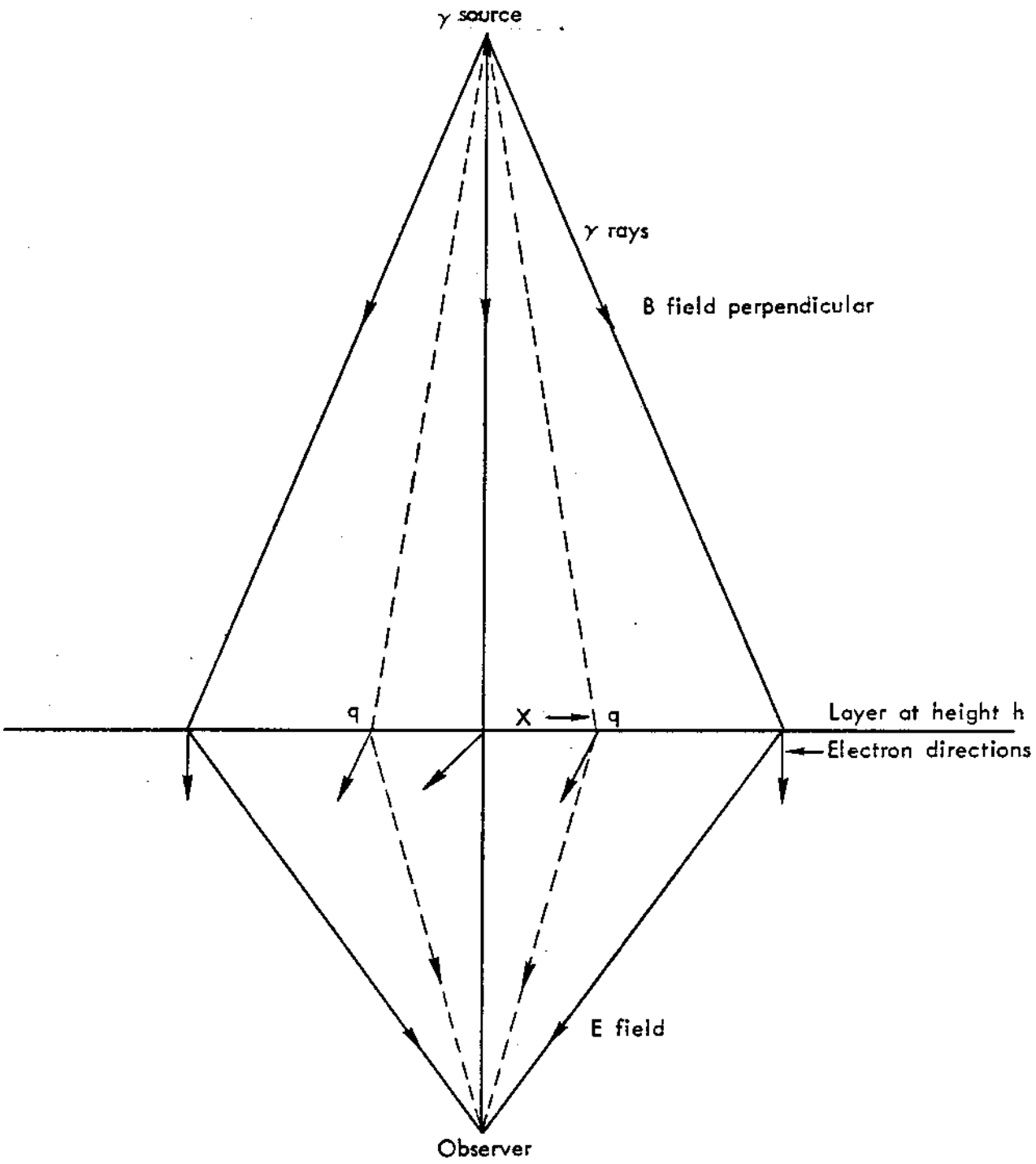

Fig. 6 — Sketch illustrating electron directions which produce observer field at time τ

It is straightforward to calculate all needed information about the initially forward-directed electron of known energy in a specified magnetic field as a function of time after its birth. The needed information is simply the variable parameters involved in the Lienard-Wiechert potential relation. Since the electrons have initial velocities near the velocity of light, the calculations must be made relativistically, by properly relating electron time and motion to observer time. Consider again electron "q." To determine its contribution to the observer field at observer time τ, we need the Lienard-Wiechert parameters for the electron at time $\Delta\tau$, where $\Delta\tau$ is in observer time. In general, we need the Lienard-Wiechert potential for observer times from zero to whatever length of time the EMP signal characteristics are to be calculated. Such calculations are easily done by computer. Figure 7 shows the normalized Lienard-Wiechert potential of an electron of velocity 0.87C (appropriate for a 1.6-MEV γ source) moving in a field of 0.6 gauss (perpendicular to the electron velocity vector) as a function of observer time. Note that, after 1.5 shakes, the field contributed by the electron is negative compared with the field from 0 to 1.5 shakes.

B. ILLUSTRATIVE CALCULATION USING A DELTA-FUNCTION γ SOURCE AND IDEAL CIRCULAR-ORBIT ELECTRONS

Using Fig. 7, we can easily determine the observer field due to the thin layer of Compton electrons illustrated in Fig. 6. Consider Fig. 8, in which the abscissa is the distance from the burst/observer axis and the ordinate is the normalized contributions from electrons in the disc to the observer field. Again, to illustrate the approach, the electrons are considered to have ideal circular orbits (atmospheric scatter, absorption, and energy conservation effects on the ideal solution will be considered subsequently) and a delta-function source of γ radiation is assumed. Figure 8 illustrates the situation for two observer times arbitrarily taken as 1 shake and 4 shakes for a burst altitude of 100 km and for the Compton electrons in a thin layer at 30 km altitude. To the observer, the total field contributed per unit density of Compton electrons in the disc is simply

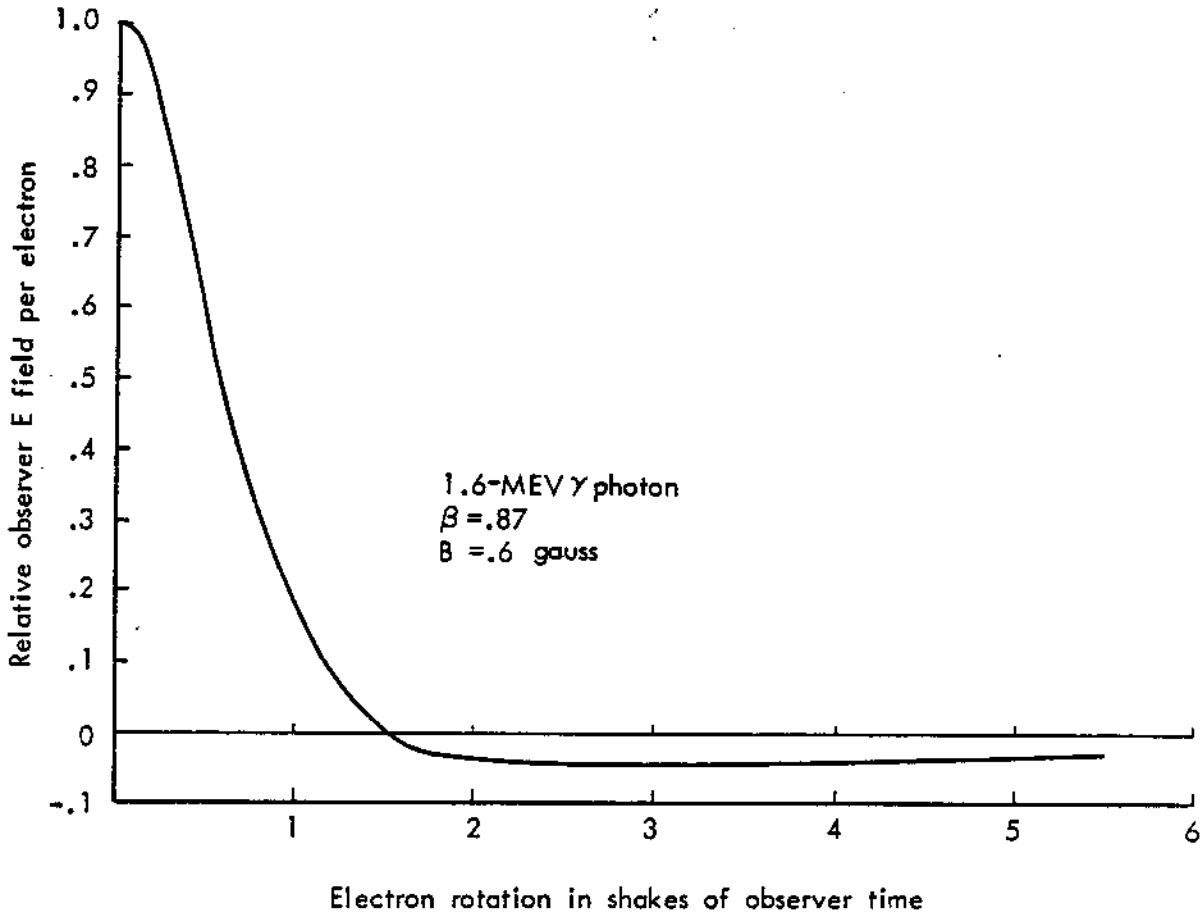

Fig. 7 — Lienard-Wiechert relative E field vs electron rotation time

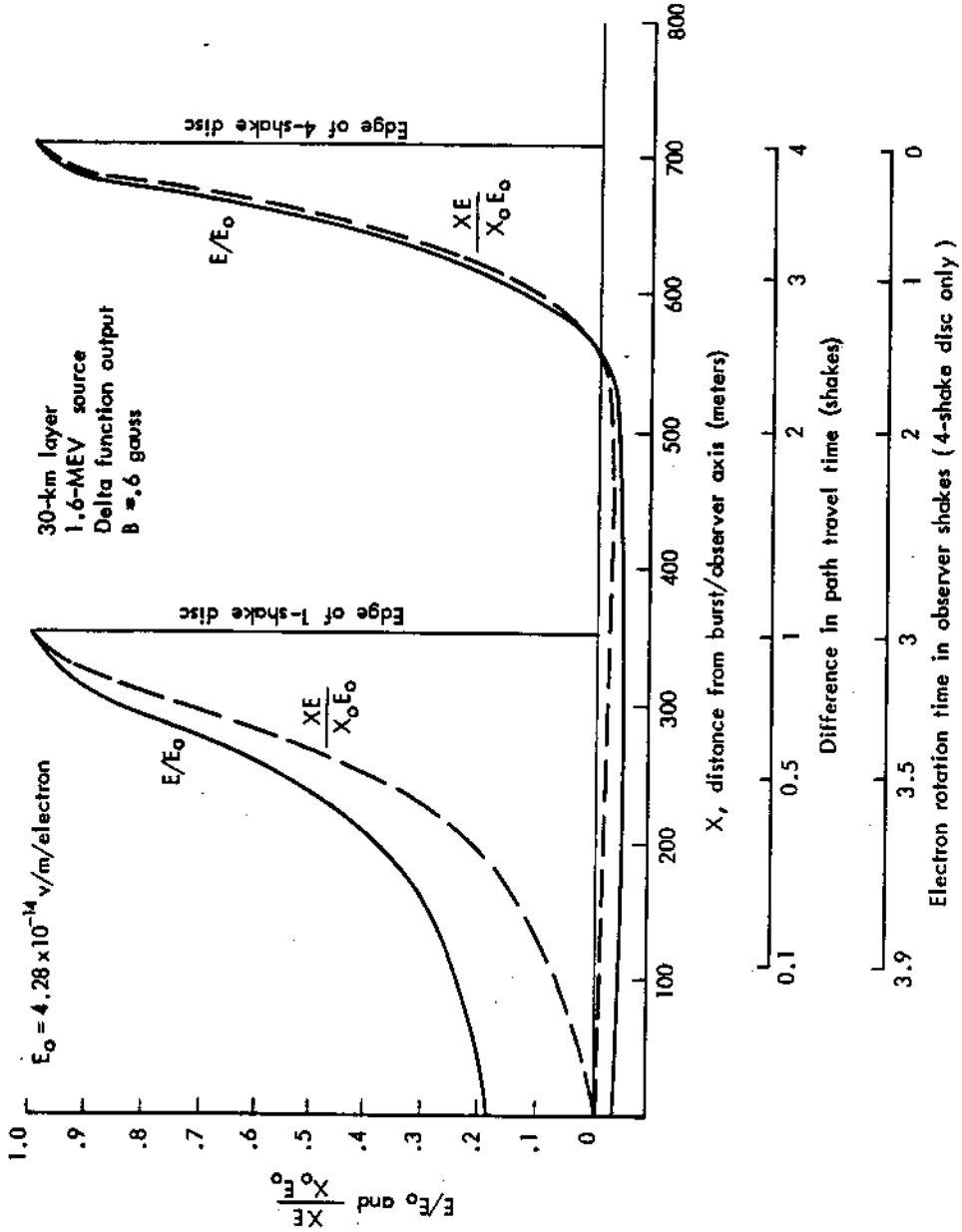

Fig. 8 – Radiation distribution at 1 and 4 shakes from electrons at 30-km altitude

$$E_T = 2\pi X_o E_o \int_o^{X_o} \frac{XE}{X_o E_o}\, dX \qquad (3)$$

or $2\pi X_o$ (maximum field intensity per electron) (area under the XE/X_oE_o curve). The maximum field intensity per electron, E_o, is simply the synchrotron field as determined by the Lienard-Wiechert expression (Eq. (2)) for the electron directed toward the observer ($\theta = 0$). For $\beta = 0.87$, $B = 0.6$ gauss, and $r = 30$ km, $E_o = 4.28 \times 10^{-14}$ v/m/electron. For the 4-shake disc in Fig. 8, the area under the XE/X_oE_o curve is 51.2 unit-meters. Thus the observer field at 4 shakes contributed by the layer of Compton electrons at 30 km is $2\pi \times 710$ m $\times 4.28 \times 10^{-14}$ v/m/electron $\times$ 51.2 m = 9.8×10^{-9} volt-meters/electron $\times$ (density of Compton electrons). From Fig. 2, for example, at 30 km the Compton electron density produced by a 0.01-KT source of γ radiation is shown to be 1.3×10^{11} electrons/m^2/km. Thus, the contribution to the observer field from the thin layer at 30 km is

$$E/h = 9.8 \times 10^{-9} \text{ volt-meters/electron} \times 1.3 \times 10^{11} \text{ electrons/m}^2\text{/km}$$

or

$$E/h = 1274 \text{ v/m/km, where h is the layer thickness in km.}$$

Following the same procedure for the 1-shake disc of Fig. 8, we obtain 1294 v/m/km.

By repeating the above procedure at other altitudes we can determine the contribution per unit height at the desired time throughout the region containing Compton electrons. Finally, the total field at the observation point at a given time is

$$E = \int_0^H E/h\, dh \qquad (4)$$

where H is the burst height.

Figure 9 shows the results at a time of 4 shakes for the geometry of Fig. 1 and a γ yield of 0.01 KT. The field intensity as calculated by the procedure leading to Fig. 9 is the ideal upper limit field

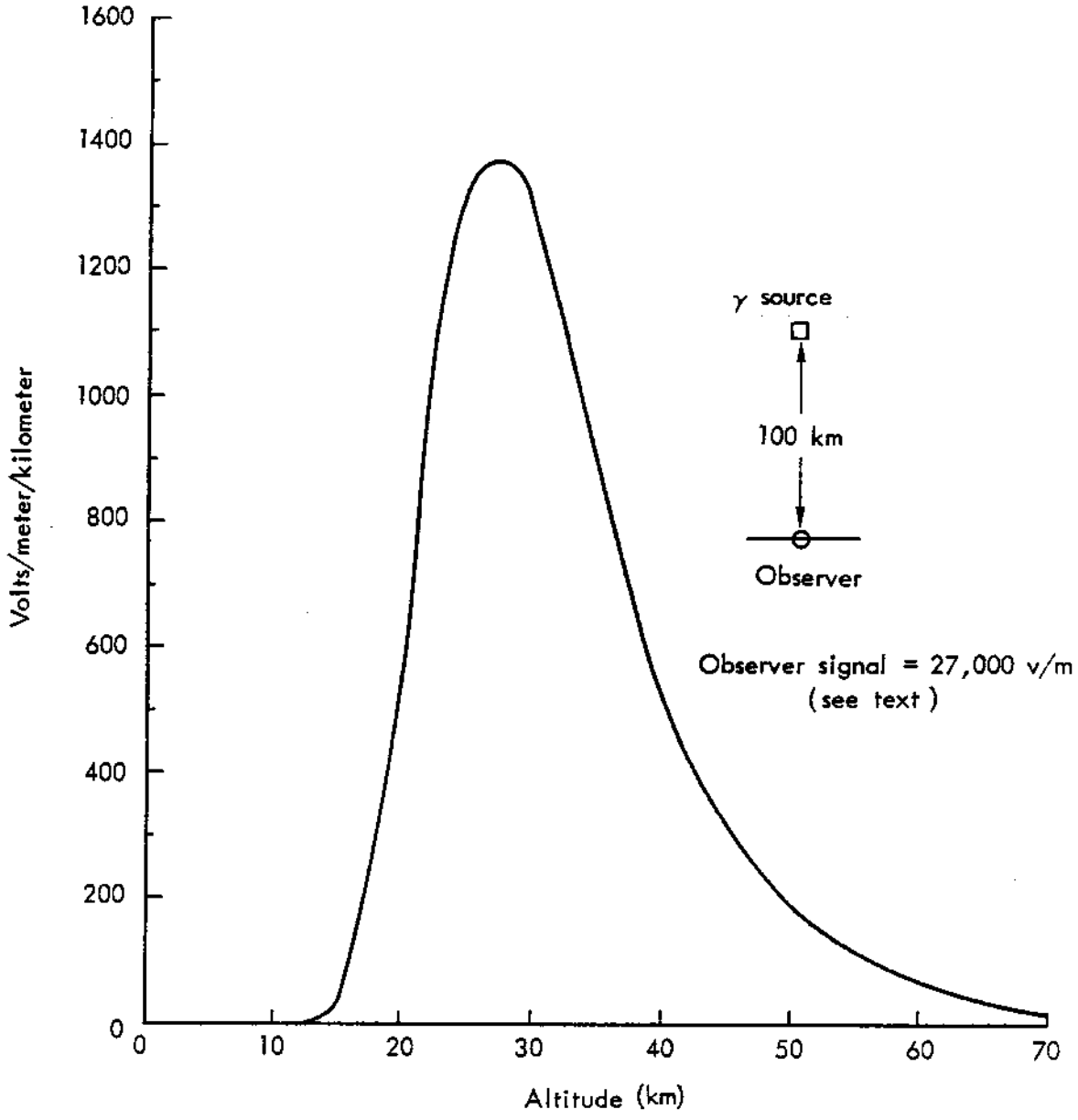

Fig. 9 — Observer signal contributions versus height at 4 shakes

producible at 4 shakes by the source, geometry, and magnetic field used. If atmospheric scattering and absorption due to ambient atmospheric ionization were negligible, for the low γ output used, the numerical value for field intensity would be reasonably close at the time shown (4 shakes) to the correct field, since other neglected factors are of minor consequence; however, addition of atmospheric scattering effects alone, as will be shown, can greatly reduce the field calculated for ideal circular orbits. Thus, practical meaning should not be attributed to the calculated field of Fig. 9. Meaningful values considering all necessary inputs to the calculation are presented later. The above material, it is believed, has adequately described the essential mechanics of the summed electron-field approach. In examination of Fig. 8, we see, for example, that at 4 shakes the observer field arises primarily from electrons in an annulus near the outer edge of the 4-shake disc. Actually, in the portion of the disc between the burst/observer axis and about 0.8 of the disc radius, radiation from the electrons tends to reduce the observer field. This physical insight into the nature of the EMP source is a valuable feature of the summed electron-field approach.

C. TIME-DEPENDENT γ SOURCE CALCULATIONS

We next examine the effect on the above solution for ideal circular-orbit electrons of a source that emits γ radiation over a period of many shakes. For convenience in illustrating the effect of a time-dependent source, we will assume an output rate that increases linearly to a maximum at 2 shakes and decreases linearly to zero between 2 and 8 shakes. We will outline the approach for handling a time-dependent γ source and illustrate the approach by calculating the observer field at 4 shakes using such a source. Consider again Fig. 6. Since the time for which the observer field is to be evaluated is less than the time during which γ radiation is being emitted by the source, at all distances from the burst/observer axis, electrons will be found having deflections appropriate for electron ages between zero and 4 shakes or less. At the outer edge of the disc the electrons have zero age but their number is also zero. At some intermediate position on

the disc (such as "q" in Fig. 6), the electron will have ages between zero and $\Delta\tau$ (as is explained on p. 12). Thus, to obtain the field contributed by electrons at, say, "q", one must convolve the γ rate output-versus-time curve with Fig. 7 to obtain the effective field contributed by the electrons of various ages. Figure 10 illustrates this process for locations on the disc where the excess travel times at the velocity of light between the source and the observer are 1 and 3 shakes. At these locations the maximum ages of electrons contributing to the observer signal at 4 shakes are 3 shakes and 1 shake, respectively. The effective E source, at any location in the disc, is readily determined by the procedure illustrated in Fig. 10. At any location on the disc in terms of the abscissa time of Fig. 10, it is simply the ratio of the area under the convolved curves (labeled a $\times$ b) to the total area under the relative γ rate curve (b). Thus at 3 shakes in Fig. 10 the ratio is 0.138. Figure 11 shows for an observer signal time of 4 shakes the relative contribution to E as a function of disc delay time as obtained by this procedure. Clearly the procedure is applicable to any arbitrary γ output rate-versus-time relation. Graphical convolution can be quickly and accurately performed.

Figure 12 shows, for the same conditions as Fig. 8, the parameters determining the radiation from the thin disc at 30 km for the time-dependent γ source illustrated in Fig. 10. Using the calculations previously given in connection with Fig. 8 for an observer time of 4 shakes, we can readily determine the disc contribution for the time-dependent γ source illustrated. The field is merely the field calculated in Fig. 8 multiplied by the ratio of the area under the XE/X_oE_o curves of Fig. 12 and Fig. 8. This ratio is $\frac{33.1}{52.1}$ or 0.635. Comparison of Fig. 8 with Fig. 12 brings out the difference in the physical electromagnetic signal generation regions at the same observer time for a delta-function γ source and for the time-dependent γ source. In Fig. 12 the principal contributing region is about 500 m from the burst/observer axis, and for Fig. 8 the principal contributing region is at the edge of the disc. The other differences are apparent.

The total field intensity at the observation point is determined by repeating the procedure for Fig. 12 at several heights in the source

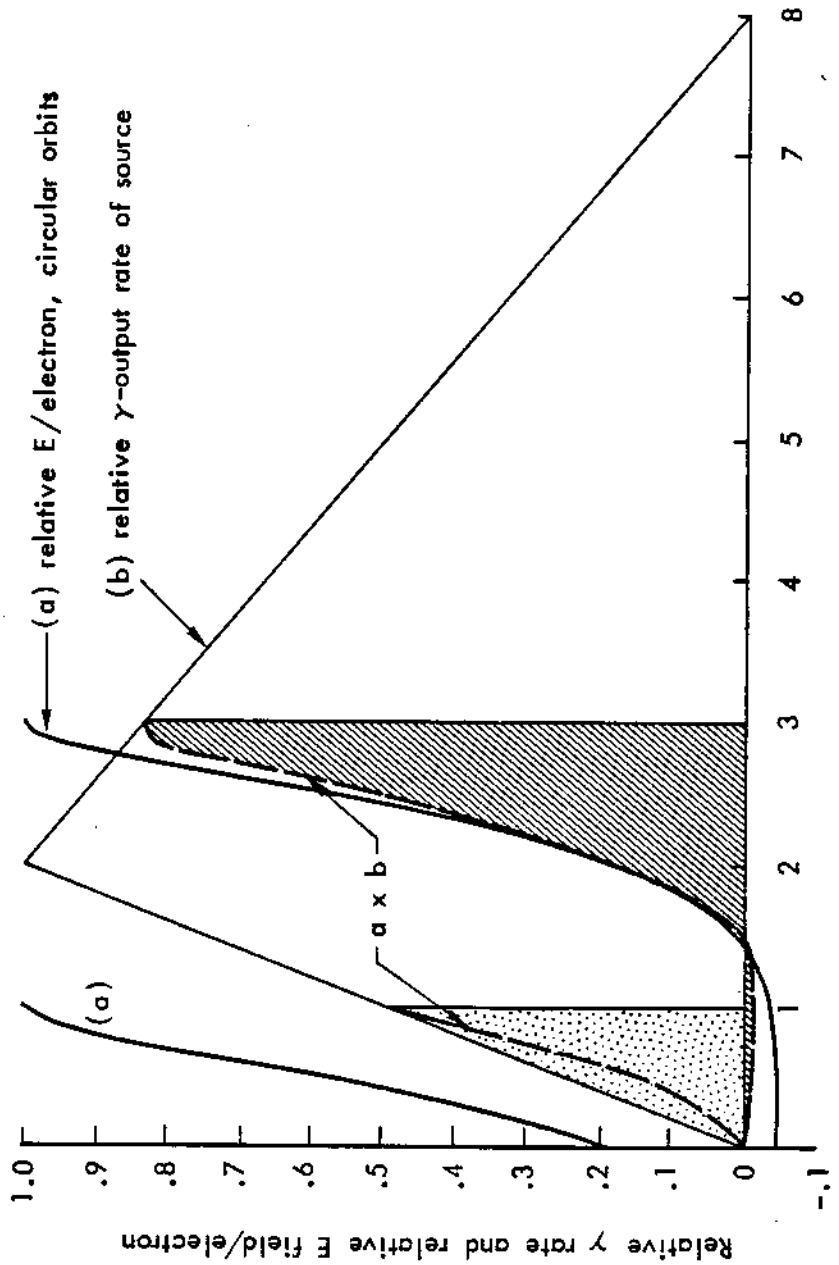

Fig. 10—Illustration of convolving γ output rate with electron field to obtain effective source at 1 and 3 shakes

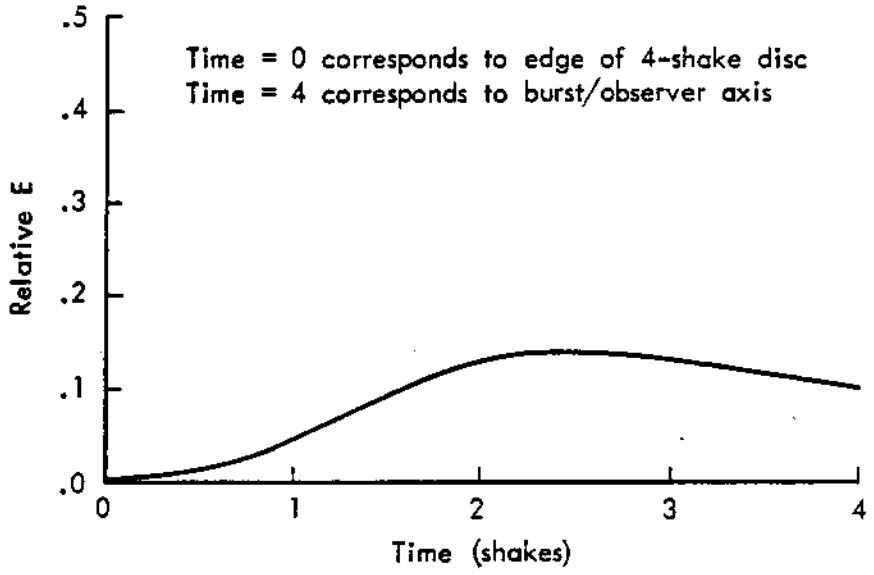

Fig. 11 — Effective electron radiation vs time for time-dependent γ source of Fig. 10

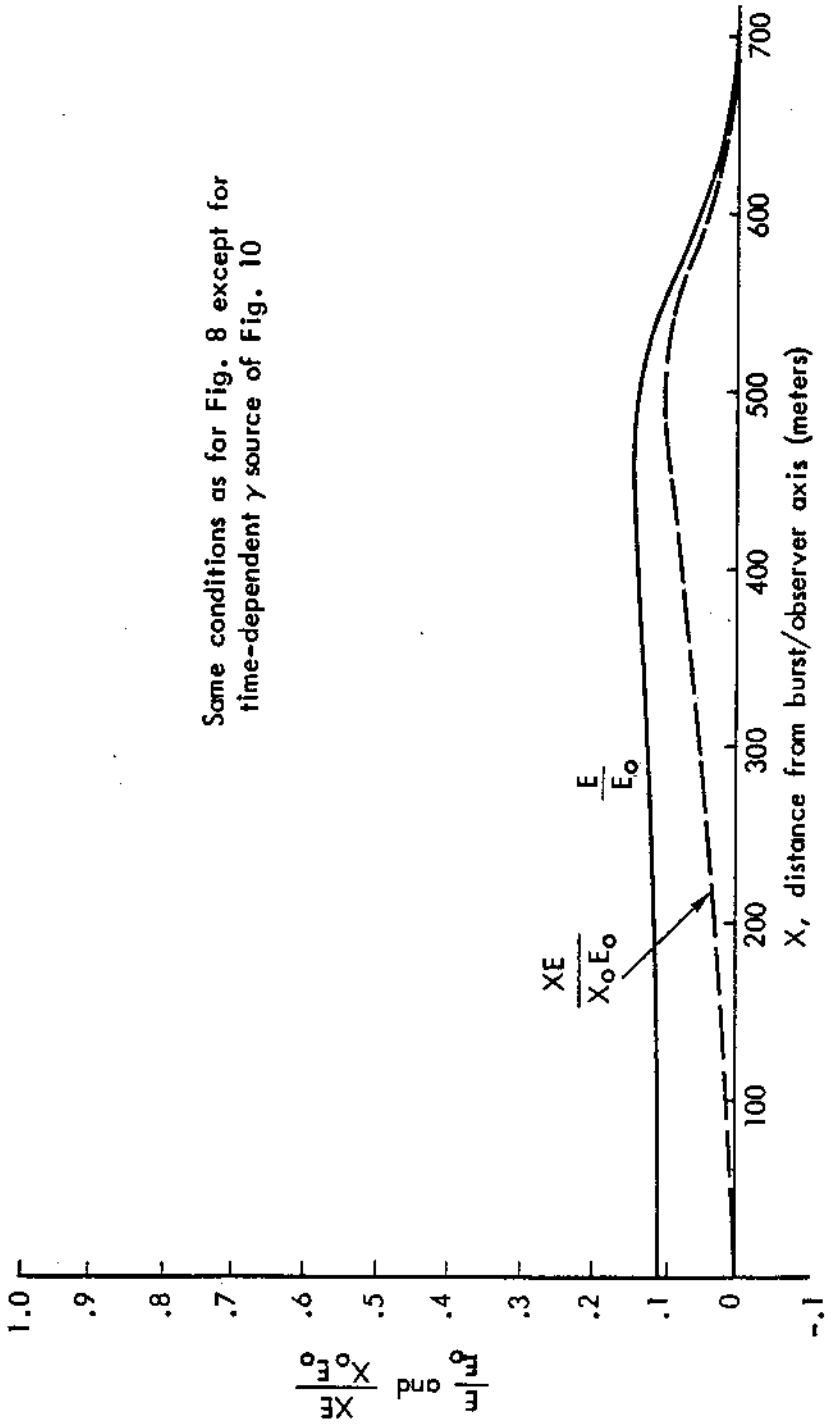

Fig. 12 — Radiation distribution at 4 shakes from electrons at 30 km altitude (time variable $\dot{\gamma}$)

region defining a curve similar to that of Fig. 9 for the delta-function source. Results of this procedure are not detailed here; however, the v/m/km curve versus height is essentially the same as that given in Fig. 9, except that the amplitude is uniformly reduced by a factor of 0.635. Thus the total observer field at 4 shakes is essentially 0.635 of that calculated (Fig. 9) for the delta-function source, or 17,000 v/m for a total γ output of .01 KT. Again, practical meaning should not be given this calculated field value, since omitted factors, subsequently considered, greatly reduce the actual expected signal.

D. EFFECTS OF INCLUSION OF ATMOSPHERIC SCATTERING OF COMPTON ELECTRONS

Next we will proceed to a more meaningful solution by including the effect of atmospheric scattering in the field calculations. Instead of the individual electrons following ideal circular orbits and producing a high degree of coherence in the summed field contributions, the electron directions rapidly become gaussianly distributed about the circular track they would follow if not scattered. The mean squared angle of scatter, θ_s^2, is proportional to the distance, D, traveled by the Compton electron after birth and is given approximately* by

$$\theta_s^2 = \frac{0.5\ D}{(E_{MEV})^2} \frac{\rho}{\rho_o} \tag{5}$$

where D is in meters

ρ is the density at the electron altitude

ρ_o is sea level density.

If the electrons were indeed initially forward-directed with an equivalent energy, E_{MEV}, as proposed on p. 8, scattering effects could be much more easily evaluated than in Compton scattering, where the electrons have a distribution of energies and initial directions relative to the direction of the incident γ radiation. Figure 13 illustrates

*Fermi[9] uses a factor of 0.7 instead of 0.5, but for electron energies near 1 MEV, the original work of Ref. 10 indicates the value 0.5 as more reasonable.

in a general way the importance of scattering in deflecting the electron from the ideal circular orbit and, hence, in reducing coherence. For Fig. 13, electrons are considered to be initially forward-directed with an energy of 0.8 MEV (β = .92). At 20 km, for example, the rms scatter angle becomes large relative to the magnetic turning angle, θ_m, at very early times. For the typical parameters illustrated, the electron, in the absence of scatter, contributes a positive field to the observer for about 1 shake, whereas with scattering effects included, the rms scatter angle reaches the zero field value in 0.1 shake at 20 km. This does not mean that the field is zero in 0.1 shake, since the fields of all the electrons in the gaussian distribution will still contribute a positive value; however, it indicates the nature of the effect. We have approximated the full scattering effect for various altitudes and electron parameters using both the continuum-current approach and the summed electron field approach.

By summing the electron fields of all the electrons in the gaussian distribution using the Lienard-Wiechert potential theory discussed on p. 8 we have derived the results of Fig. 14 for 1.6-MEV γ radiation and a perpendicular magnetic field of 0.6 gauss. Figure 14 shows the relative E field contributed by the average Compton electron (in the Klein-Nishina distribution) as a function of time for altitudes of 20, 30, and 40 km. Also shown is the relative E field per electron based on the parameters of the circular-orbit forward-directed electron discussed on p. 10. Figure 14 illustrates the severe effect at 20 km of scattering in reducing the effective electron radiation and also shows that the scattering at 40 km is relatively small but not negligible. It is clear that neglect of scatter in EMP calculations can lead to sizable overestimates of the calculated fields, as originally shown in Refs. 3 and 4.

Results derived for the relative E field, as a function of electron age for the various altitudes of interest, can be incorporated into the analysis directly. If the γ source were a delta function, instead of using Fig. 7 for obtaining the disc distribution of Fig. 8, we would use the scatter curve for the appropriate altitude as illustrated in Fig. 14. For a time-dependent source, it is necessary to convolve

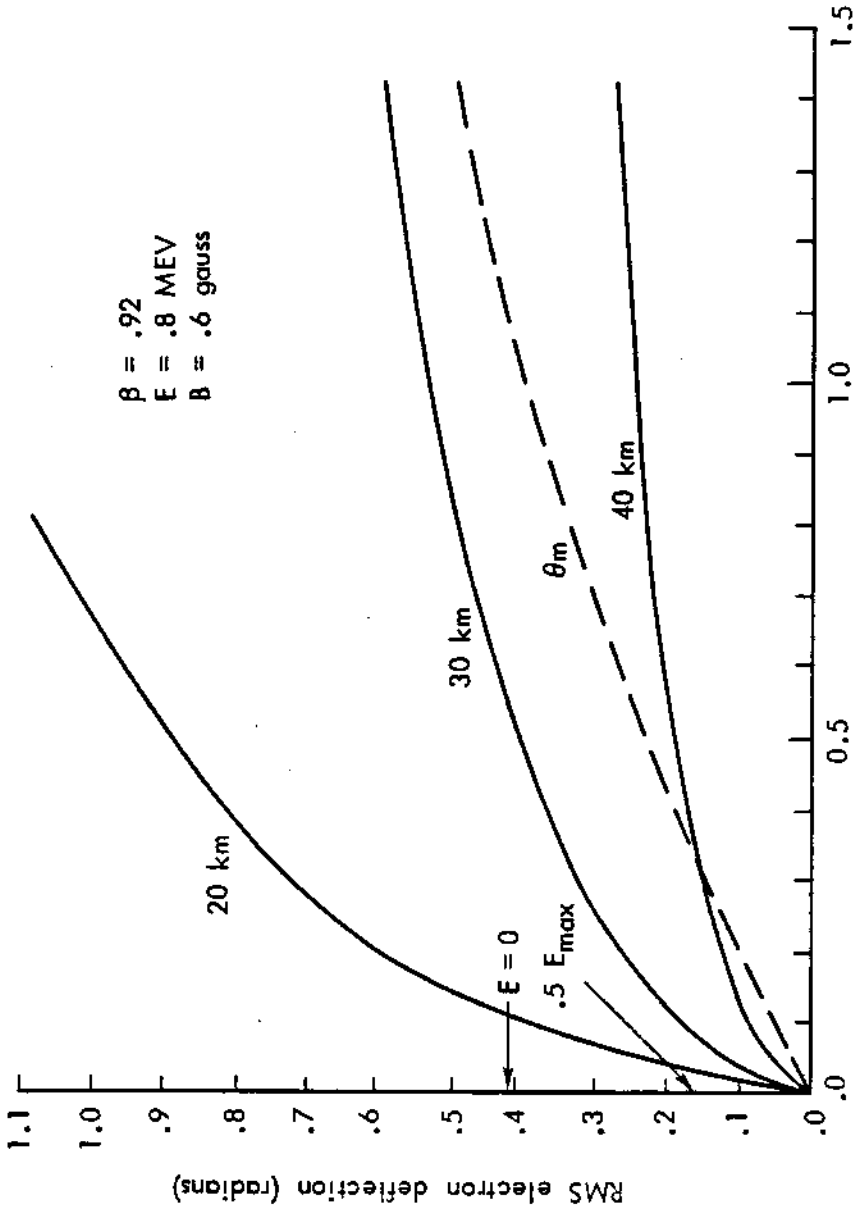

Fig. 13 — Electron deflection vs time due to scattering and to magnetic field

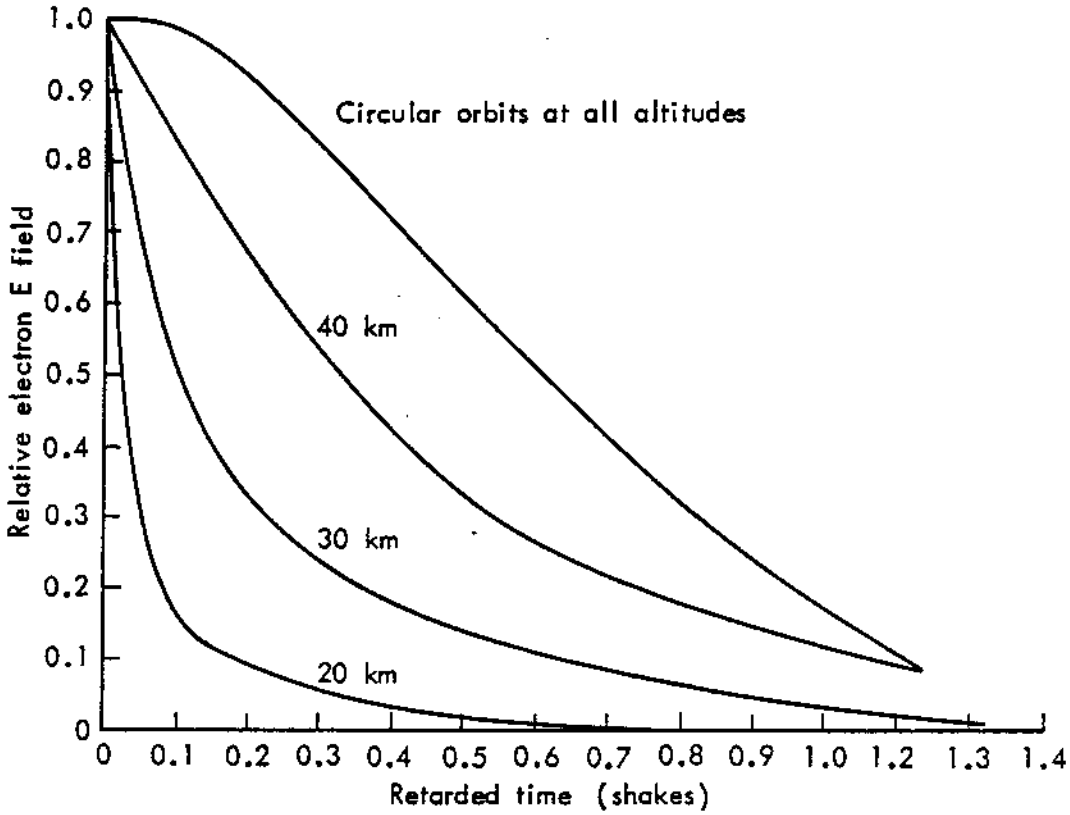

Fig. 14 — Relative electron field versus time with scattering

the relative E curve (with scatter) for the altitude of interest, such as those shown in Fig. 14, with the γ rate curve (as was illustrated in Fig. 10 for the case of ideal circular orbits) in order to determine the contribution to the observer field from a given disc location at a given time. Figure 15 shows the results of convolving the relative E field of the ensemble of scattered Compton electrons with the γ output rate illustrated in Fig. 10. It shows (as a function of time after the first γ radiation arrives at any point in the γ deposition region) the relative E field contributed to the radiation field by the average scattered electron in this region. At $\tau = 0^+$, the electrons contribute their maximum radiation field (or a relative field of 1.0) at all altitudes, with or without scatter. New Compton electrons continue to appear for a duration equal to that of the source pulse, and electrons of increasing age contribute decreasing radiation depending on the altitude of the disc. Thus the net result is a curve which decreases from a value of 1.0 to zero over a time somewhat longer than the duration of γ radiation from the source. Figure 15 shows the average Compton electron contributions that have been made at the times shown; at 2 shakes, for example, for the pulse illustrated in Fig. 10, only 0.25 of the Compton electrons have been produced, and these electrons at 20 km produce an average field per electron 0.086 of the initial field from the forward-directed electron.

Using results as illustrated in Fig. 15 and the procedure detailed for Fig. 8, we can proceed to evaluate the upper limit of the observer field considering a time-dependent γ source and including atmospheric scatter. Still not included in the calculation at this stage are absorption effects and energy conservation. Figure 16 shows the distribution of the E field source from the center to the edge of the 1- and 4-shake thin discs (i.e., the discs at 30 km that contribute to the 1- and 4-shake observer E field) previously illustrated in Fig. 8 for a delta-function source and with scattering neglected. Table 1 details the calculated parameters used in plotting Fig. 16. In comparing Figs. 8 and 16, note that the vertical scale of Fig. 16 is 0.1 the scale of Fig. 8. Also plotted in Fig. 16 is the result for no scatter, previously shown in Fig. 12 for the 30-km thin layer contribution

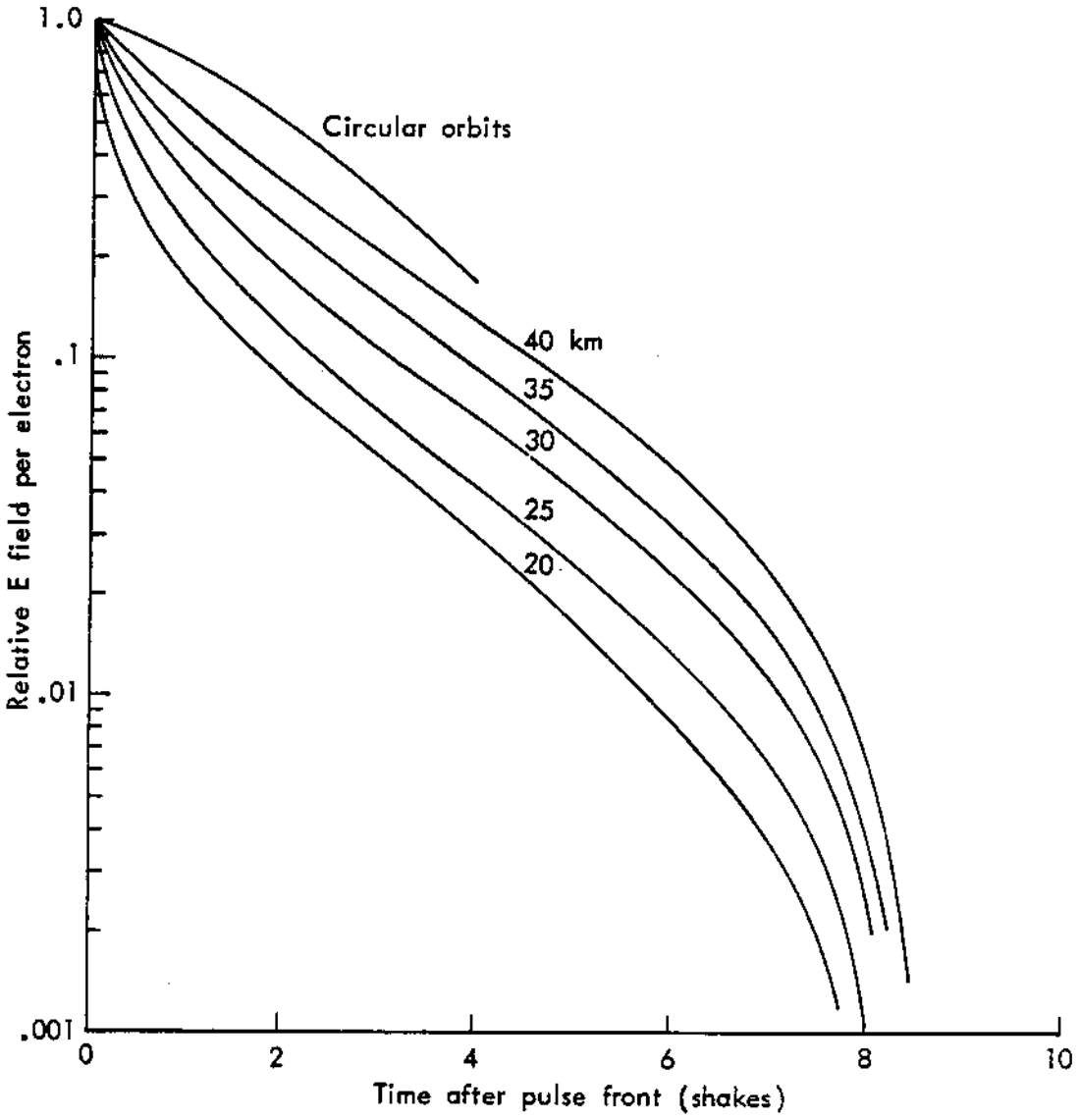

Fig. 15 — Convolved scatter (Fig. 14) and time-dependent $\dot{\gamma}$ source (Fig. 10)

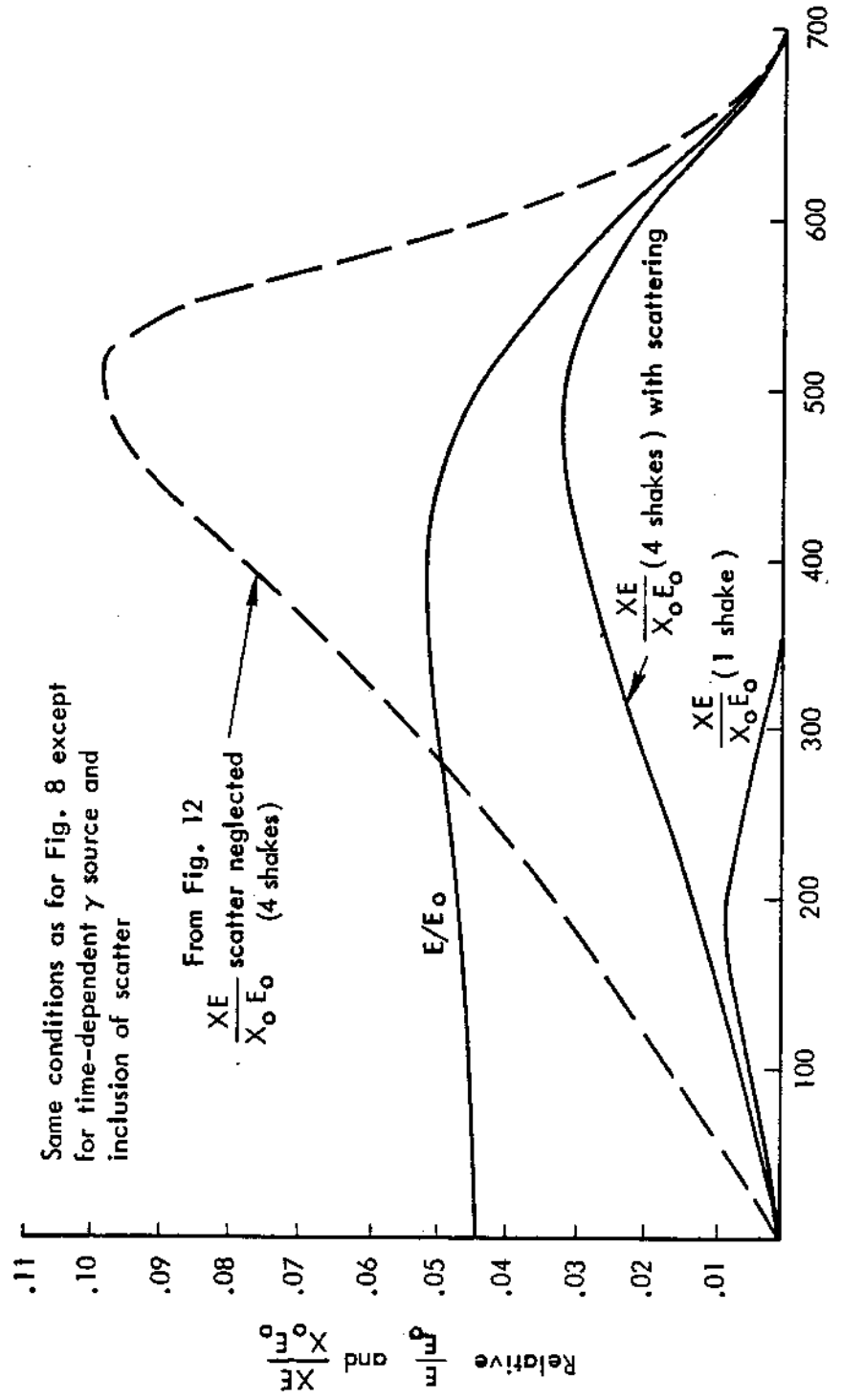

Fig. 16 — Radiation distribution at 1 and 4 shakes from electrons at 30-km altitude

to the observer field at 4 shakes. The area under the XE/X_oE_o curve is proportional to the intensity of the observer field in units of v/m/km. The ratios among areas in the three cases considered in Fig. 8, Fig. 12, and Fig. 16 are as follows (at 4 shakes):

$$\frac{\text{Fig. 16 - Scatter and time-variable } \gamma \text{ source}}{\text{Fig. 12 - No scatter and time-variable } \gamma \text{ source}} = 0.41$$

$$\frac{\text{Fig. 16 - Scatter and time-variable } \gamma \text{ source}}{\text{Fig. 8 - No scatter and delta-function } \gamma \text{ source}} = 0.26$$

Table 1

NUMERICAL VALUES FOR THE DISC AT 30 km CONTRIBUTING TO THE RADIATED E FIELD AT THE OBSERVER LOCATION AT 4 SHAKES OBSERVER TIME (τ = 0 is instant of arrival of first signal)

a	b	c	d	e	f	g
Path Delay to Position on Disc (shakes)	Time after Arrival of Gamma Front (shakes)	Radial Distance from Burst/ Observer Axis (meters)	Relative Convolved E (per electron)	Fraction of Compton Electrons Made	E/E_o	XE/X_oE_o
0	4.0	0	.066	.672	.0443	0
0.5	3.5	251	.083	.578	.0483	.0171
1.0	3.0	355	.108	.479	.0517	.0259
1.5	2.5	435	.137	.370	.0507	.0311
2.0	2.0	502	.180	.250	.0450	.0318
2.5	1.5	561	.246	.141	.0338	.0267
3.0	1.0	615	.335	.0625	.0209	.0181
3.5	.5	664	.52	.0156	.0081	.0076
4.0	0	710	1.0	0	0	0

NOTES:

Column f = Column e × Column d
Column g = Column f × Column c × $1/X_o$

X_o = 709 meters (Eq. (1))

Using the same numerical factors previously derived for the 30-km layer (p. 17), we obtain 1274 × 0.26 or 331 v/m/km for the 30-km disc's contribution to the observer EMP signal at 4 shakes in observer time.

By repetition of the above procedure, the 30-km disc contribution at 1 shake is determined to be only 19 v/m/km compared to 1294 v/m/km for the delta source and neglecting scatter (Fig. 8). In the time interval 0 to 2 shakes, it is apparent that the contribution of the disc to the observer field increases closely proportionally to $(\text{time})^3$. With a delta-function γ source, the signal increases with $(\text{time})^1$, and with a linearly increasing time-variable γ source the number of contributing electrons increases with $(\text{time})^2$; thus the signal amplitude is proportional to $(\text{time})^3$. At 1 shake after arrival of the first γ photons for the γ time output rate assumed, as shown in Table 1, only 0.0625 of the first-scatter Compton electrons which are ultimately produced (i.e., in 8 shakes) have been produced on the burst/observer axis and none have been produced at the edge of the contributing 1-shake disc. The above time characteristics are the same throughout the height range of the radiating Compton electrons; thus the total EMP signal produced by integration of the contribution of all the thin layers throughout the height region containing Compton electrons has the same amplitude-versus-time behavior at early times. For a given total γ yield from the source, the rise characteristics of the radiated EMP depend, in general, on both (1) the rate of increase of the γ output rate and (2) the total time over which a given γ output is produced.

E. EFFECTS OF INCLUSION OF ABSORPTION EFFECTS FROM RESIDUAL IONIZATION AND SELF-IONIZATION

General

Ionization between the radiating electron sources and the observer will reduce the radiation, as was previously calculated in this Note and illustrated in Fig. 16. In the summed electron-field method of calculating EMP signals, the effect of this intervening ionization is calculated by use of standard propagation theory and analysis procedures. The field contributed by a given electron is reduced by the integrated

attenuation in the path between the electron and the observer at the proper time. Two sources of ionization, must, in general, be included: (1) ionization which existed in the region between the electron and the observer prior to the creation of the Compton electrons whose radiation is to be determined and (2) secondary ionization produced by the Compton electrons by inelastic collisions with the atmospheric gases. The first source, preionization, can be considered independent of time for times of interest in EMP problems. The second source, self-ionization, has an involved time-and-space dependence, which must be evaluated.

Figure 17 shows an expanded view of Fig. 1 for the region between 30 km and the observer. Boundaries of the ellipsoids for differential path delays between the source and the observer of from 0 to 4 shakes are shown.

Consider again the radiation from the thin layer at 30 km which contributes to the total observer field at 4 shakes, as illustrated in Fig. 16 for the case of a time-dependent γ output and including atmospheric scatter effects on the Compton electron radiation. Electron radiation from the edge of the 4-shake disc that contributes to the 4-shake observer field traverses path "a" in Fig. 17 from the 30-km height to the observer; hence the reduction in signal contributed at the observation point from the edge of the disc is determined by the integrated differential absorption along path "a." Preionization will be essentially constant for EMP times of interest at a given altitude in any practical situation. Self-ionization at a given altitude is determined by the length of time Compton electrons have existed at the altitude. Along path "b", the burst/observer axis, Compton electrons have existed for 4 shakes independent of height below 30 km. Along path "a", however, the maximum time Compton electrons have existed and, hence, have been producing secondary electrons, is much less. For example, path "a" penetrates the 25-km height at a point where the path delay (from burst to observer at the velocity of light) is about 3.1 shakes. Thus the signal contributed to the observer field at 4 shakes from the edge of the disc encounters self-ionization accumulated over 4 - 3.1 (or 0.9) shakes, but along the burst/observer axis, the radiation

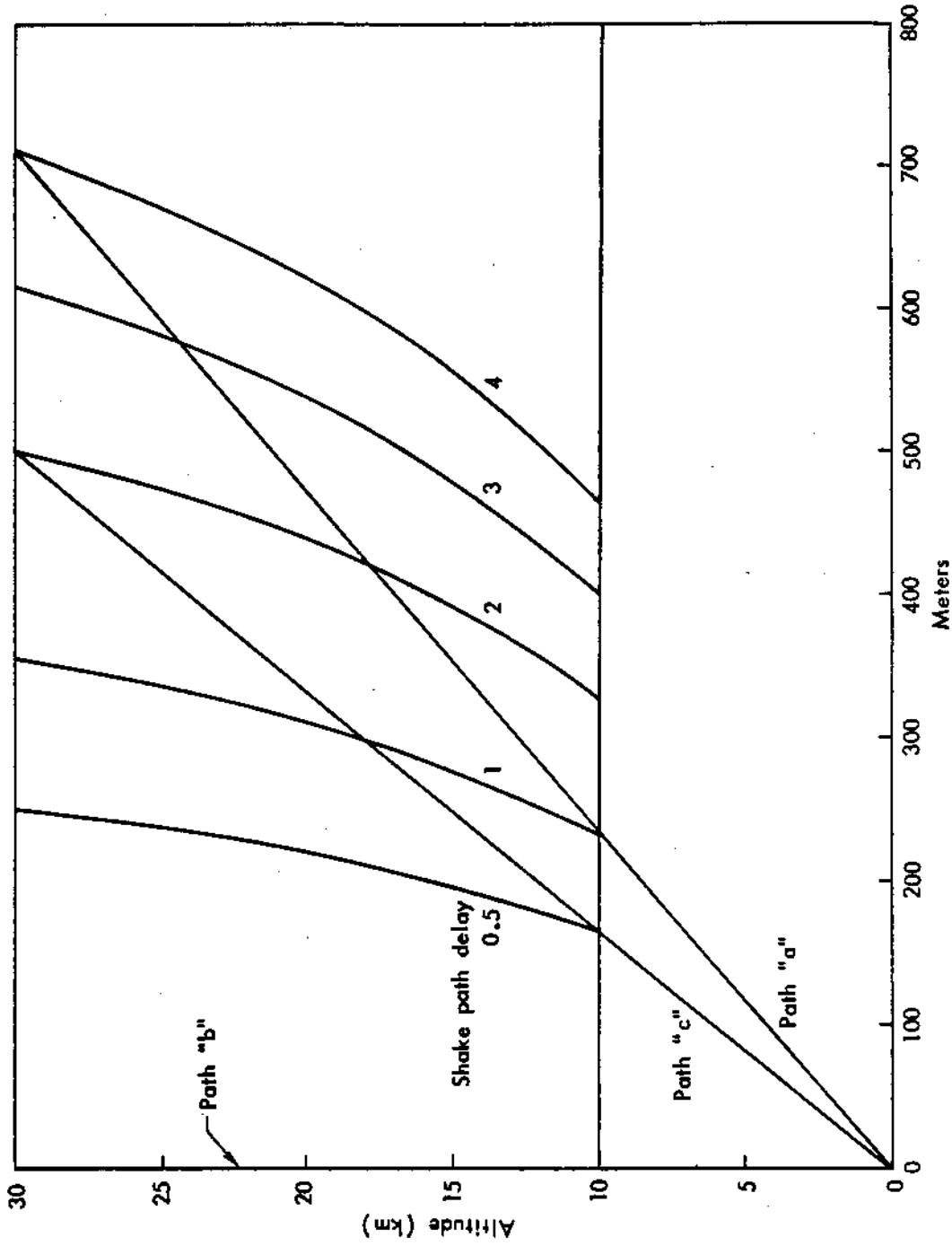

Fig. 17 — Illustrative path delay ellipsoids and geometry for absorption calculations

from electrons contributing to the observer field at 4 shakes encounters self-ionization, which has built up for 4 shakes. As a further illustration, consider path "c." Radiation from the 30-km disc contributing to the observer field at 4 shakes is attenuated by the self-ionization created in 2 shakes at the 30-km height and about 4 - 1.6 (or 2.4) shakes at 25 km. The differences in absorption at a given time for radiation from various portions of the disc may appear to cause computational complexity; however, it will be shown to be relatively easily handled.

Absorption Due to Self-Ionization

To determine absorption produced by self-ionization along any path from the disc to the observer we first determine the electron density as a function of altitude and time after the arrival of the γ radiation front. At the given altitude and time, ionization at all portions of the disc is the same, since the disc radius is much smaller than the distance from the burst to the disc; the time (in the observer's frame of reference) at which ionization builds up to a given value increases with radial distance on the disc from the burst/observer axis, as illustrated by the path delay curves in Fig. 17. Since the time history of first-scattered Compton electrons produced at a given altitude is known from a prescribed weapon γ yield and γ time history, the magnitude of the secondary ionization produced by the Compton electrons approximated can be as a function of time, considering the effects of atmospheric scattering [11] and ionization lag, [12] i.e., the nonzero time required for Compton electrons to produce low-energy secondary electrons. In Ref. 11, the problem was simplified by assuming that the high-energy electrons were initially foward-directed and that the electron energy was consumed in producing secondary ionization; to date no secondary ionization-versus-time calculations appear to have been published which use the full Klein-Nishina distributions of electron energy and electron direction as a point of departure and in addition account for energy loss to the electromagnetic field system. Such calculations, even for monoenergetic γ radiation, are considerably more complex numerically than calculations using "equivalent" forward-

directed electrons. Figure 18, based on material presented in Ref. 11, shows the fraction of secondary electrons produced as a function of observer time for a forward-directed 0.742-MEV electron at 20-km altitude. At times of principal interest, i.e., at less than about 8 shakes (since scattering has essentially randomized the Compton electron source for periods this long for altitudes below 40 km, as shown in Fig. 15), Fig. 18 may be applied to other altitudes between about 15 and 35 km by scaling by a factor ρ/ρ_{20}, where ρ is relative density at altitude h, by including a correction for ionization lag as given in Ref. 12, and by scaling with energy as given by Evans.[5]

To obtain the fractional secondary-electron density at a given altitude for a time-dependent source of γ radiation, we must convolve the fractional ionization versus time (as illustrated in Fig. 18 for 20 km altitude) with the source γ rate-versus-time curve (as illustrated in Fig. 10). Figure 19 illustrates the convolution of Fig. 10 and Fig. 18 and shows the result for the fraction of secondary electrons produced at 20 km versus time for the γ output rate of Fig. 10. The fraction applies to the total of secondary electrons produced by the first-scatter Compton electrons, which are shown as the curve N_1 in Fig. 2.

By the procedure illustrated in Fig. 19, we can determine the density of secondary electrons produced by Compton electrons as a function of time for any altitude in the γ deposition region. Figure 20 shows the densities at several altitudes for a 0.01 KT γ output at 100 km altitude.

Having determined the secondary-electron density as a function of time and altitude, we can calculate the absorption of the electron radiation propagated to the observer, expressed in dB/km. Since the conductivity of a given density of secondary electrons (i.e., σ/n) is a function of the existing electric field intensity[13] and since the field intensity is to be calculated, it is initially necessary to estimate the field intensity. For the estimated field value and the electron density values previously calculated, we can calculate the resulting conductivity and absorption and proceed, as will be detailed, to calculate the observer field. The observer's location can be either

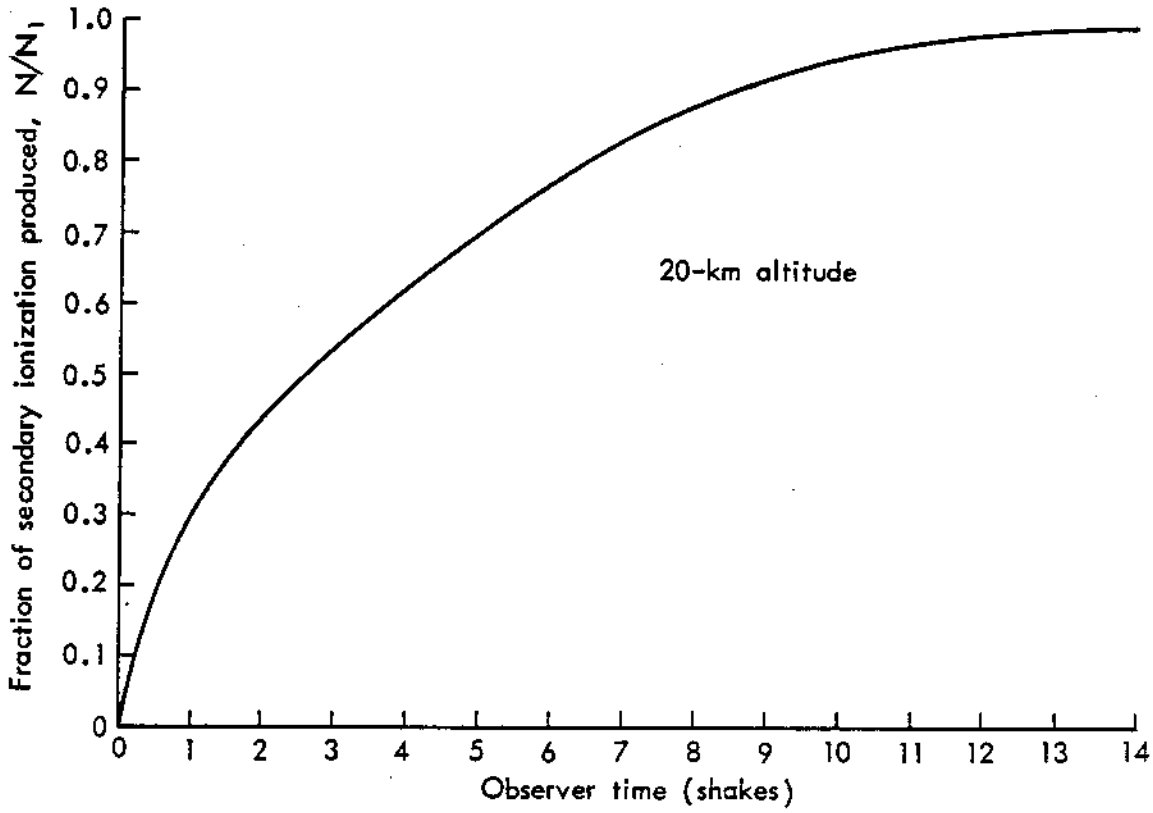

Fig. 18—Fraction of secondary electrons from first Compton electron versus time

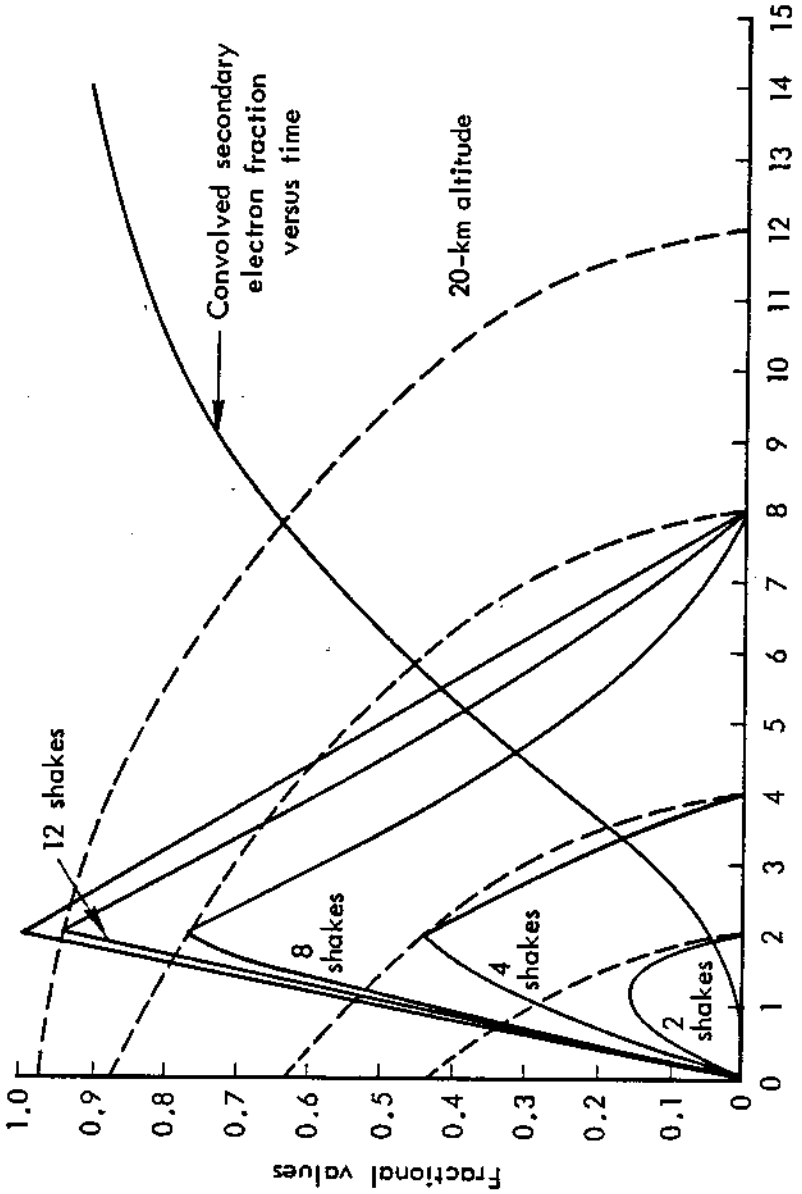

Fig. 19— Fraction of secondary electrons produced versus time for time-dependent $\dot{\gamma}$ source (Fig. 10)

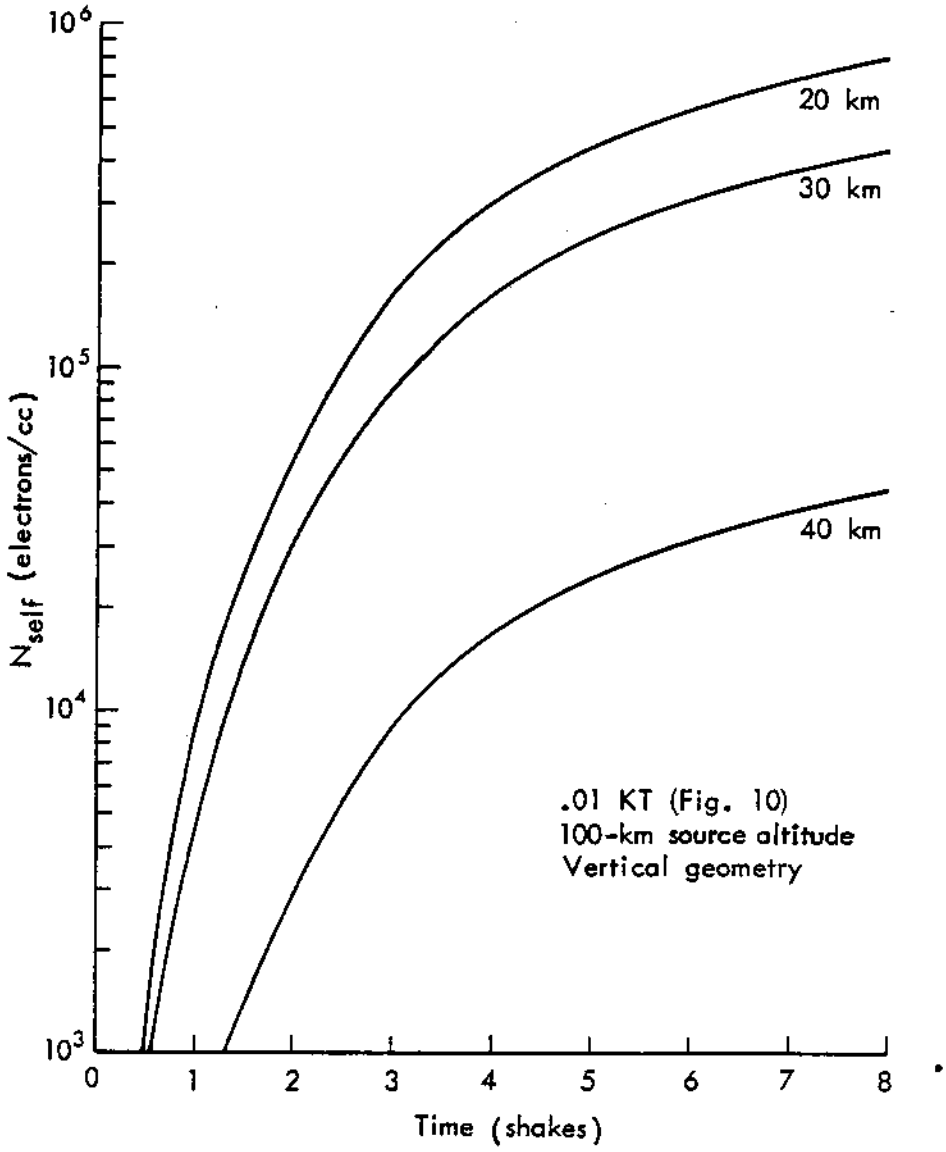

Fig. 20 — Electron density due to first-scatter Compton electrons

within the Compton source region or external, as illustrated in Fig. 1. It turns out that the field in the principal source region can be quite adequately approximated by simple inverse distance scaling. Thus, at 30 km altitude for the geometry of Fig. 1, the field will be about $\frac{100}{70}$ times the observer field.

If we are satisfied with determination of a conservative upper-limit estimate of the magnitude of the observer EMP field, the numerical complexity arising from the field-dependent conductivity problem can be avoided by using a constant minimum conductivity per electron, which is determined by the maximum field intensity value (and thus a minimum of absorption) at the appropriate altitude in the source region. After evaluation of the observer field for the assumed conductivity, we may refine the solution as desired by an iterative procedure, i.e., a new estimate of conductivity is based on the first calculated field and the same procedure followed with the new estimate to obtain an improved calculated field, and so forth. For the dB/km calculations of Table 2, a conductivity value 1/20th of the value commonly used for low fields was assumed; hence, the dB/km values for a given electron density are simply 1/20th of that deduced in Ref. 14. This low value of effective conductivity is appropriate for electric fields of about 20,000 v/m at 20 km altitude.[15] Hence, if the solution using this value produces indicated peak fields of, say, 5000 v/m, we have underestimated absorption at 20 km altitude, and iteration of the solution with a properly increased conductivity will reduce the 5000 v/m initial calculation value.

Inspection of Table 2, which is based on a γ output of 0.01 KT, indicates that self-absorption is small throughout the height range of 20 to 40 km. Thus the solution previously illustrated (Fig. 16 and pp. 29-31) will not be greatly affected by inclusion of self-absorption. For example, the signal contributed to the observer field at 4 shakes by electrons on the disc at a radial distance of 500 meters (2-shake maximum age) in Fig. 16 turns out to be attenuated less than 1 dB.

Table 2

DIFFERENTIAL ABSORPTION FOLLOWING A 0.01 KT DETONATION AT 100 km--VERTICAL GEOMETRY

Time After γ Front Arrival (Shakes)	dB per Path Kilometer		
	20	30	40
	Altitude (km)		
0	0	0	0
1.0	4.4×10^{-3}	1.0×10^{-2}	8.0×10^{-3}
2.0	2.5×10^{-2}	6.0×10^{-2}	2.9×10^{-2}
3.0	7.2×10^{-2}	1.7×10^{-1}	9.0×10^{-2}
4.0	1.4×10^{-1}	3.2×10^{-1}	1.7×10^{-1}
6.0	2.5×10^{-1}	6.1×10^{-1}	3.1×10^{-1}
8.0	3.6×10^{-1}	8.5×10^{-1}	4.4×10^{-1}

F. SUMMARY COMMENTS ON SUMMED ELECTRON-FIELD METHOD

This section has discussed in detail the procedure for calculating the contribution to the observer field at any specified time from a thin layer in the Compton electron source region. The method of calculation and the thread of a numerical example were presented together in a step-by-step approach to make the procedure as clear as possible as well as to provide a better feeling for the comparative aspects of the (1) delta-function versus time-variable γ source, (2) effect of inclusions of atmospheric scatter in the calculations, and (3) effect of preionization, when present, on the field calculations. The final objective is, of course, to specify for a given geometry and burst parameters the electromagnetic signal amplitude versus time characteristics. To complete this objective, the analyst merely performs several calculations of the type given to produce Fig. 16, modified as appropriate to include preionization absorption, when present. Exactly the same procedure for finding the contribution to the observer field illustrated for the thin disc at 30 km is repeated at other altitudes in the Compton electron source region, and the results are integrated over height. This procedure, repeated at a number of observer times, thus determines the volts/meter at the observation point as a function of time. All the numerical procedures required for this total solution have been brought out in this section. Although vertical geometry was used for ease of illustration, the method is identical for oblique paths if we neglect the minor inaccuracy brought about by the fact that the disc, as used for vertical geometry, will be tilted for oblique burst/observer geometry. Because different portions of the disc are at different altitudes, the circular symmetry for disc calculations used for vertical geometry is not strictly correct; however, for disc sizes up to a few kilometers, the simplifying assumption of circular symmetry about the burst/observer axis is, for practical purposes, quite adequate.

The procedure outlined in this report leads to "upper-limit" calculated pulse values because of omission of two factors. These are (1) full energy conservation considerations and (2) effects of the fields of the pulse itself on the orbits and hence on the radiation of

the individual electrons. Our work has indicated that calculations which omit these factors and produce calculated fields under 10,000 v/m are little affected (i.e., reduced in amplitude) by their inclusion; hence the values illustrated in this section, while upper limit in nature for the assumed parameters, are essentially the same as would be obtained by including the additional factors with their sizable computational complexity. Final accuracy of the result is limited more by basic parameters, such as conductivity, knowledge of the state of atmospheric ionization at the time of burst, and scatter evaluation.

REFERENCES

1. Karzas, W. J., and R. Latter, *Phys. Rev.* 137, B 1369, 1965.

2. Sollfrey, W., private communication, September 1973.

3. Booker, H. G., private communication, June 1973.

4. Sollfrey, W., *Analytic Theory of the Effects of Atmospheric Scattering on the Current and Ionization Produced by the Compton Electrons from High-Altitude Nuclear Explosions*, The Rand Corporation, R-1973-AF, October 1977.

5. Evans, R. D., *The Atomic Nucleus*, McGraw Hill Book Company, New York, 1955.

6. *U.S. Standard Atmosphere 1962*, U.S. Government Printing Office, Washington, D.C.

7. Panofsky, W. K. H., and Melba Phillips, *Classical Electricity and Magnetism*, Addison-Wesley Publishing Company, Reading, Massachusetts, 1955.

8. Sollfrey, W., private communication, 1973.

9. Fermi, E., *Nuclear Physics*, The University of Chicago Press, Chicago, 1950.

10. Williams, E. J., *Proc. Roy. Soc.*, A169, S31, 1939.

11. Knutson, G. R., *The Effect of Nuclear-Coulomb Electron Scattering on High Altitude EMP Sources*, Air Force Weapons Laboratory, Theoretical Note #161, February 1972.

12. Longmire, C., and H. J. Longley, *Improvements in the Treatment of Compton Current and Air Conductivity in EMP Problems*, Mission Research Corporation, Report MRC-N-2, Santa Barbara, California, 1971.

13. Engelhardt, A. G., A. V. Phelps, and C. C. Risk, *Phys. Rev.* 135, No. 6A, 1964.

14. Knapp, W. S., and P. G. Fischer, *Aids for the Study of Electromagnetic Blackout*, Defense Nuclear Agency, Report No. DASA 2499, General Electric TEMPO, Santa Barbara, California, 1970.

15. Canavan, G. H., J. E. Brau, and L. A. Wittwer, *Self-Consistency, Mobility, and Cascading in High Altitude EMP Calculations*, draft report, Air Force Weapons Laboratory, 1973.